Meteoritics & Planetary Science 38, Nr 2, 269–292 (2003)
Abstract available online at http://meteoritics.org

Yamato 86029: Aqueously altered and thermally metamorphosed CI-like chondrite with unusual textures

Eric K. TONUI,[1, 2*] Michael E. ZOLENSKY,[2] Michael E. LIPSCHUTZ,[3]
Ming-Sheng WANG,[3] and Tomoki NAKAMURA[4]

[1]California Institute of Technology, Division of Geological and Planetary Sciences, Mail Code 170–25, Pasadena, California 91125, USA
[2]NASA Johnson Space Center, Astromaterials Research and Exploration Science (ARES), Mail Code ST, Houston, Texas 77058, USA
[3]Department of Chemistry, Purdue University, West Lafayette, Indiana 47907–1393, USA
[4]Department of Earth and Planetary Sciences, Faculty of Sciences, Kyushu University, Hakozaki, Fukuoka 812-8581, Japan
*Corresponding author. E-mail: etonui@gps.caltech.edu

(Received 15 May 2002; revision accepted 4 November 2002)

Abstract–We describe the petrologic and trace element characteristics of the Yamato 86029 (Y-86029) meteorite. Y-86029 is a breccia consisting of a variety of clasts, and abundant secondary minerals including coarse- and fine-grained phyllosilicates, Fe-Ni sulfides, carbonates, and magnetite. There are no chondrules, but a few anhydrous olivine-rich grains are present within a very fine-grained phyllosilicate-rich matrix.

Analyses of 14 thermally mobile trace elements suggest that Y-86029 experienced moderate, open-system thermal metamorphism. Comparison with data for other heated carbonaceous chondrites suggests metamorphic temperatures of 500–600ºC for Y-86029. This is apparent petrographically, in partial dehydration of phyllosilicates to incompletely re-crystallized olivine. This transformation appears to proceed through 'intermediate' highly-disordered 'poorly crystalline' phases consisting of newly formed olivine and residual desiccated phyllosilicate and their mixtures. Periclase is also present as a possible heating product of Mg-rich carbonate precursors.

Y-86029 shows unusual textures rarely encountered in carbonaceous chondrites. The periclase occurs as unusually large Fe-rich clasts (300–500 μm). Fine-grained carbonates with uniform texture are also present as small (10–15 μm in diameter), rounded to sub-rounded 'shells' of ankerite/siderite enclosing magnetite. These carbonates appear to have formed by low temperature aqueous alteration at specific thermal decomposition temperatures consistent with thermodynamic models of carbonate formation. The fine and uniform texture suggests crystallization from a fluid circulating in interconnected spaces throughout entire growth. One isolated aggregate in Y-86029 also consists of a mosaic of polycrystalline olivine aggregates and sulfide blebs typical of shock-induced melt re-crystallization.

Except for these unusual textures, the isotopic, petrologic and chemical characteristics of Y-86029 are quite similar to those of Y-82162, the only other heated CI-like chondrite known. They were probably derived from similar asteroids rather than one asteroid, and hence may not necessarily be paired.

INTRODUCTION

Type CI carbonaceous chondrites have elemental abundances closest to those of the solar photosphere and are therefore regarded as the most primitive Solar System material available for study (Anders and Grevesse 1989; Burnett et al. 1989). These meteorites consist largely of fine-grained phyllosilicates, which account for most of the water (~20 wt% H_2O). They also lack chondrules and rarely contain inclusions of anhydrous silicates. Carbonates and sulfates are also common. The CI chondrites are interpreted as the end products of an extended period of aqueous alteration on hydrous asteroids (e.g., Zolensky and McSween 1988; Tomeoka 1990b; Zolensky, Bourcier, and Gooding 1989c). Oxygen isotope compositions require that such alteration occur at low temperatures (~140ºC) and high water-to-rock

ratios (3.56) corresponding to a volume fraction of water of ~80% (Clayton and Mayeda 1984). Precise knowledge of the constituent minerals is of great importance in deciphering the details of these processes in these primitive meteorites. However, CI chondrites are very rare compared with other carbonaceous chondrites, and hence study of a new sample is pregnant with possibilities.

Petrological characteristics of Yamato 86029 (Y-86029) are typical of CI chondrites but bulk oxygen isotopic composition (Mayeda and Clayton, personal communication 2002) is similar that of thermally metamorphosed carbonaceous chondrites Y-82162, Y-86720, Y-86789, and B-7904 (Clayton and Mayeda 1999). Absence of bulk chemical abundances for non-volatile elements precludes a complete CI classification at this stage, although we will treat it as one for the purposes of this paper. It is only the second CI-like chondrite recovered from Antarctica, yet no comprehensive description of it exists in literature. Its predecessor, Y-82162, and the other carbonaceous chondrites mentioned above show effects of thermal metamorphism in their parent asteroids (Paul and Lipschutz 1989, 1990; cf., Wang and Lipschutz 1998). Hence, it is essential to analyze in Y-86029 the highly mobile trace elements (using radiochemical neutron activation analysis or RNAA) that act as thermometers for such metamorphic events (cf., Wang and Lipschutz 1998; Lipschutz, Zolensky, and Bell 1999). Y-86029 also contains unusual textures that have rarely been reported in carbonaceous chondrites.

In this paper, we present the results for isotopic, petrologic and trace element chemistry of Y-86029 in order to: 1) classify its bulk composition; 2) examine its petrography and unusual textures; and 3) determine the genesis and relationship among its components. Unusual carbonaceous chondrites like Y-86029 and others such as LEW 85332 (Brearley 1997; Tonui, Zolensky, and Lipschutz 2002a), ALH 85085 (Scott 1988; Weisberg, Prinz, and Nehru 1988), and Kaidun (Zolensky et al. 1996) continue to provide an important source of information regarding the diversity of materials that formed in the early solar system and highlight the fact that these materials are not as pristine as earlier thought.

ANALYTICAL METHODS

Y-86029 weighs 11.83 g. We examined both existing thin sections of Y-86029 provided by the National Institute of Polar Research (NIPR) in Tokyo. We analyzed mineral grains and matrix in all samples for major elements using a CAMECA SX100 microprobe operated at 15 kV and 20 nA. We used a focused beam (~2 μm) for anhydrous mineral grains and a defocused beam (10 μm) for matrix phyllosilicates. Natural mineral standards were utilized, and corrections were applied for absorption, fluorescence, and atomic number effects using the CAMECA on-line PAP program. These probe analyses are accurate to within 1%, relative for major elements. Element maps were also made using this instrument. Secondary electron and backscattered electron (BSE) images were made using a JEOL JSM-6340F field emission scanning electron microscopy (SEM), operating at 15 kV, an electric potential that offers optimum values of resolution versus electron penetration (and excitation) of the samples.

Fine-grained (mostly matrix) material was selected for more detailed characterization by transmission electron microscopy (TEM). These observations were made using ultramicrotomed sections of grains embedded in EMBED-812 low-viscosity epoxy. We observed the microtomed sections using a JEOL 2000FX scanning transmission electron microscopy (STEM) equipped with a LINK EDX analysis system, operated at 200 kV. We used natural mineral standards and in-house determined k-factors for reduction of compositional data, which are considered to be accurate only to within ±6%, relative; a Cliff-Lorimer thin-film correction procedure was employed (Goldstein 1979). In the case of phyllosilicates, mineral identifications were made on the basis of both composition and electron diffraction data whenever possible.

Approximately 50 mg of Y-86029 for RNAA analysis was sealed in quartz and irradiated with suitable monitors for four days at a flux of 8×10^{13} n $cm^{-2}s^{-1}$ at the University of Missouri Research Reactor (UMRR). Irradiation conditions, monitor preparation, chemical processing, and counting conditions were similar to those described by Wang and Lipschutz (1998). Chemical yields were satisfactory, ranging up to 92%, and exceeded 40% for all samples. Chemical yields for monitors exceeded 50% in all cases.

For the x-ray diffraction analysis, samples were mounted on a thin glass fiber 5 μm in diameter and exposed to Cr Kα synchrotron x-rays in a Gandolfi camera. The diffraction data were collected at beam line 3 A at The Photon Factory Institute of Material Science, High Energy Accelerator Research Organization (Tsukuba, Japan) and was monochromated to 2.16 Å. A clear x-ray powder photograph can be taken from a single piece of matrix of 20 microns in size with exposure duration (120 minutes for Y-86029) by the Gandolfi method (Gandolfi 1967). The x-ray photograph was scanned by a high-resolution scanner, and the read data were transferred to a computer to determine precise peak positions and integrated intensity. The relative abundance of major constituent minerals was determined on the basis of the integrated intensities of x-ray reflections (Nakamura et al. 2001).

PETROGRAPHY AND MINERALOGY

Y-86029 is a breccia consisting of millimeter to sub-millimeter clasts, anhydrous fragments, isolated minerals, and matrix (Fig. 1a). It exhibits minimal to moderate terrestrial weathering (weathering category A/B). These clasts are very fine-grained and are brownish to yellowish brown in near-

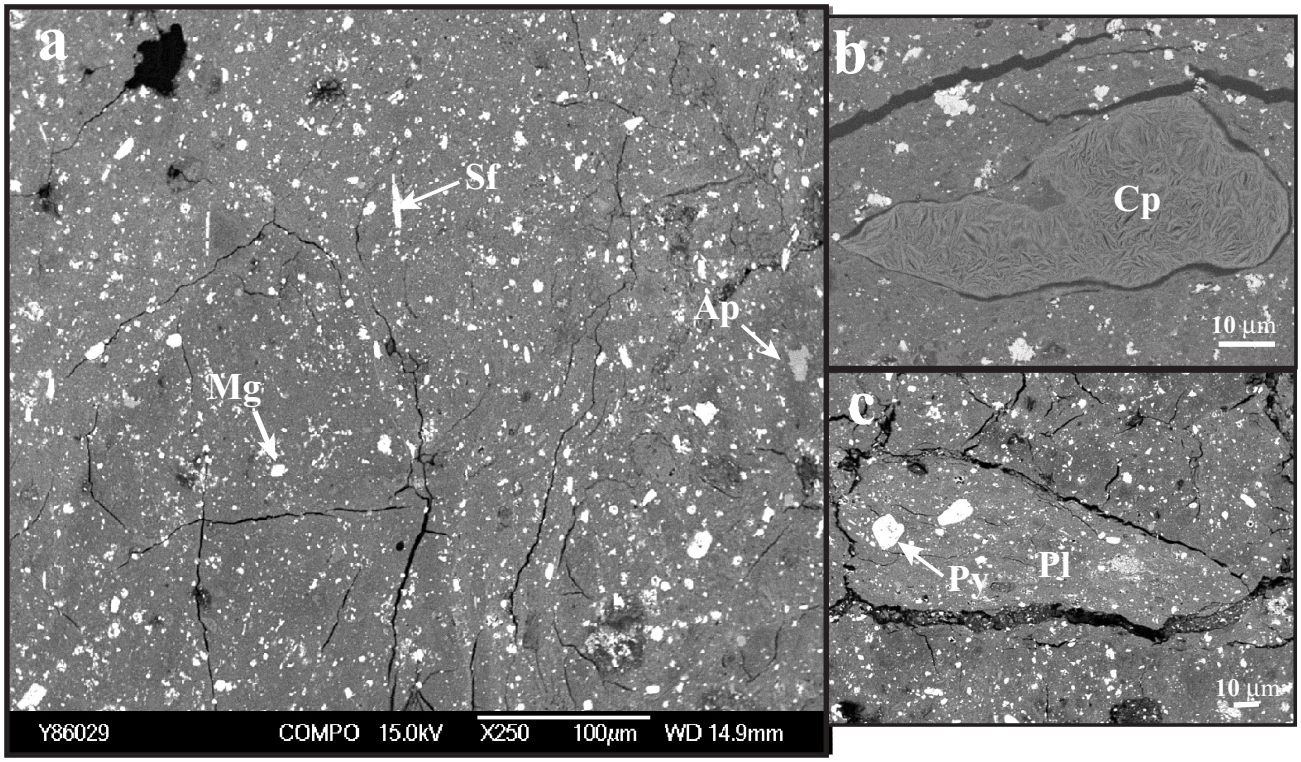

Fig. 1. Backscattered electron (BSE) images of Y-86029: a) fine-grained matrix and other secondary minerals e.g., apatite (Ap), sulfides (Sf), and magnetite (Mt); b) coarse phyllosilicate cluster (Cp) within the matrix; c) a phyllosilicate clast (Pl) with inclusions of pyrrhotite (Py) of various sizes.

translucent matrix. The color and darkness of matrix does not vary much in the thin section. Y-86029 contains no chondrules but it has abundant secondary minerals, including coarse- and fine-grained phyllosilicates, Fe-Ni sulfides, carbonates, and magnetite. No sulfates have been detected.

Phyllosilicates

Phyllosilicates make up the bulk of Y-86029 (~80 vol%) and occur as isolated coarse-grained clusters (Fig. 1b), discrete clasts (Fig. 1c), or matrix. Here, matrix is defined as fine-grained aggregates which fill the interstitial spaces among clasts or various components. The coarse-grained, isolated clusters (or 'coarse' phyllosilicates) range in size from 30 to 400 μm and make up ~10 vol% of all phyllosilicates. These clusters are yellowish brown in transmitted light and are easily distinguishable by their fibrous, anhydrous, spongy morphology. They often occur together with magnetite, pyrrhotite, and apatite, suggesting contemporaneous formation.

Microprobe analyses (Table 1) of the 'coarse' phyllosilicates (in terms of Fe, Si, and Mg) suggest they are mixtures of smectite and serpentine (Fig. 2). The analyses plot much closer to the trioctahedral smectite ideal solid solution lines as compared with the matrix phyllosicates (Fe/(Fe + Mg) ratios or fe# = 0.15–0.95; average of 0.32). These phyllosilicates contain high amounts of Na_2O (1.57–4.53 wt%) and Cr_2O_3 (0.23–3.12 wt%). The $Na_2O + K_2O$ versus Al_2O_3 contents (Fig. 3) show that these phyllosilicates plot within the range of 'sodian talc' ($Na_{0.5}Mg_6[Si_{7.5}Al_{0.5}]O_{20}$ $[OH]_4$), which forms a solid solution to talc ($Mg_6Si_8O_{20}$ $[OH]_4$) and sodium-aluminium talc ($NaMg_6[Si_7Al]$ $[OH]_4$; Schreyer, Abraham, and Kulke 1980). The higher Cr_2O_3 contents in 'coarse' rather than matrix phyllosilicates is apparent in their clustering in the Cr_2O_3 versus FeO plot (Fig. 4). Both 'coarse' and matrix phyllosilicates have high analytical totals (Table 1) as a result of partial dehydration during thermal metamorphism (see discussion).

Microprobe analysis suggests that the matrix phyllosilicates are mixtures of serpentine and smectite (Fig. 2). The discrete phyllosilicate clasts within matrix have similar compositions. These phyllosilicates have variable Fe contents (fe# is similar to those of 'coarse' phyllosilicates i.e., 0.15–0.52; average = 0.31). Elemental plots of Fe versus Si and S and Ni versus S (Fig. 5) show that these elements correlate in Y-86029 matrix suggesting that the matrix of Y-86029 is homogeneous. Sulfur shows a slightly larger variation with Ni. This is probably because of abundance of sub-micron grains of pentlandite rather than pyrrhotite.

TEM analysis shows that the matrix phyllosilicates of Y-86029 are mainly poorly crystalline, based on lattice fringes in HRTEM images and electron diffraction (SAED) patterns.

Table 1. Microprobe analyses (in wt%) of Y-86029 phyllosilicates compared with those of Y-82162 and Orgueil.

	Y-86029[a]				Y-82162		Orgueil	
Species	Coarse-1	Coarse-2	Matrix-1	Matrix-2	Coarse[b]	Matrix[c]	Coarse[d]	Matrix[e]
SiO_2	43.5	50.8	38.3	36.9	48.3	36.2	31.4	33.0
TiO_2	0	0	0.03	0.06	0.01	0.09	–	0.08
Al_2O_3	4.23	5.28	2.37	2.34	4.28	2.66	1.99	2.57
FeO	17.1	9.91	26.5	23.7	9.89	24.3	7.45	22.1
MnO	0.24	0.28	0.28	0.14	0.00	0.28	–	0.26
Cr_2O_3	1.85	1.31	0.47	0.46	1.62	0.57	0.01	0.58
MgO	27.5	24.5	24.5	25.3	27.7	24.0	31.4	19.8
CaO	0.25	0.34	0.27	0.64	0.14	0.43	–	0.29
Na_2O	2.13	2.31	0.44	0.33	2.31	0.56	–	0.05
K_2O	0.15	0.25	0.17	0.07	0.23	0.17	–	0.02
P_2O_5	0	0	0.04	0.15	0.00	0.04	–	0.08
S	0.02	0.03	0.03	0.04	1.35	2.71	0.38	1.39
NiO	0.13	0.09	2.08	1.80	0.08	2.17	0.20	2.78
Total	97.1	95.1	95.5	91.9	96.6	94.2	80.3	83.0

[a]Only analyses with S <0.05 wt% are considered for Y-86029.
[b]From Tomeoka, Kojima, and Yanai (1989).
[c]From Zolensky, Barrett, and Browning (1993); average of 50 analyses.
[d]From Tomeoka and Buseck (1988); NaO, P_2O_5, K_2O, CaO, TiO_2, and MnO together comprise only <2 wt%.
[e]From Zolensky, Barrett, and Prinz (1989b); average of 43 analyses.

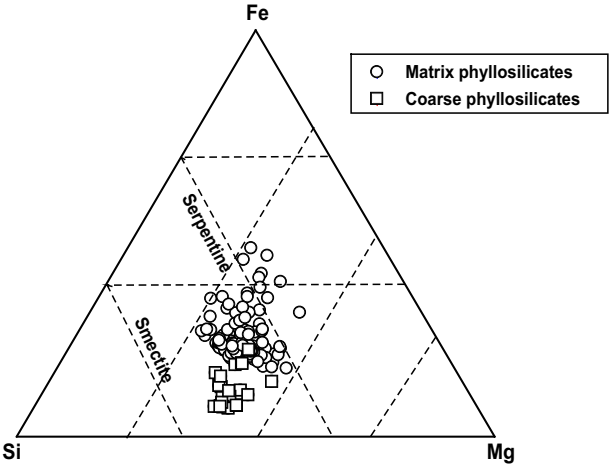

Fig. 2. Composition of matrix and coarse phyllosilicates in Y-86029 (WDS data), plotted onto a Fe-Si-Mg atom % ternary diagram.

A few thick platy phyllosilicate-like crystals (Figures 6a and 6b) are present. Regular lattice images of matrix phyllosilicates are rare, however, lattice images with highly disordered and defect structures are predominant. The patchy patterns shown in Fig. 6 correspond to these disordered and defect structures. The thick platy crystals have faint or no crystal lattices 'sandwiched' between well-developed crystal fringes. These lattices have d-spacings ranging from 9 Å to13 Å, consistent with saponite but not serpentine. Pentlandite occurs within these poorly crystalline patches as tiny (20–100 nm), rounded, very fine-grained particles. Electron diffraction (ED) patterns are composed of olivine spots and weak saponite-type spots and streaks with stacking disorders (Fig. 6b) often found in minerals that were once phyllosilicates (e.g., Akai 1988).

We encountered a few grains with well-developed crystal lattices (Fig. 7). More detailed examination, however, confirmed that these grains were not 'normal' phyllosilicates because they have d-spacings ranging from 9 Å to 9.5 Å and other fewer closely more lattices with d-spacings between 4.5 Å to 4.8 Å. They appear to be 'intermediate phases' during partial dehydration of phyllosilicates to olivine (see discussion). Apart from pentlandite, most of the other secondary minerals are not conspicuous at the TEM scale.

XRD analysis reveals that the matrix is composed of olivine, magnetite, and troilite (Fig. 8). No diffraction reflections of phyllosilicate minerals are recognized, suggesting that the crystallinity of phyllosilicate is very low. The abundance of troilite is rather surprising given that it was not detected during electron microprobe analysis, suggesting heterogeneity in distribution of sulfides. Troilite rather than pyrrhotite is commonly observed in x-ray reflections of fine-grained matrix in carbonaceous chondrites, which have been significantly heated or not extensively aqueously altered (Zolensky et al. 2002).

Anhydrous Silicates

Anhydrous silicates are generally sparse in Y-86029. We have observed two large (50–200 μm) olivine-rich aggregates Figures 9a and 9b) and a few smaller (<20 μm) aggregates (e.g., Fig. 9c). One of the aggregates (Fig. 9a; Table 2) has narrow olivine compositions (average $MgFe_{0.95}SiO_4$; $Fo_{51 \pm 3}$) and is traversed by a vein that is sprinkled with minute (<5 μm) pentlandite and pyrrhotite grains (Fig. 9b). One analysis (Table 2) indicates the presence of low Ca pyroxene ($En_{98}Fs_{1.1}Wo_{0.9}$). Parallel orientation and optical continuity of

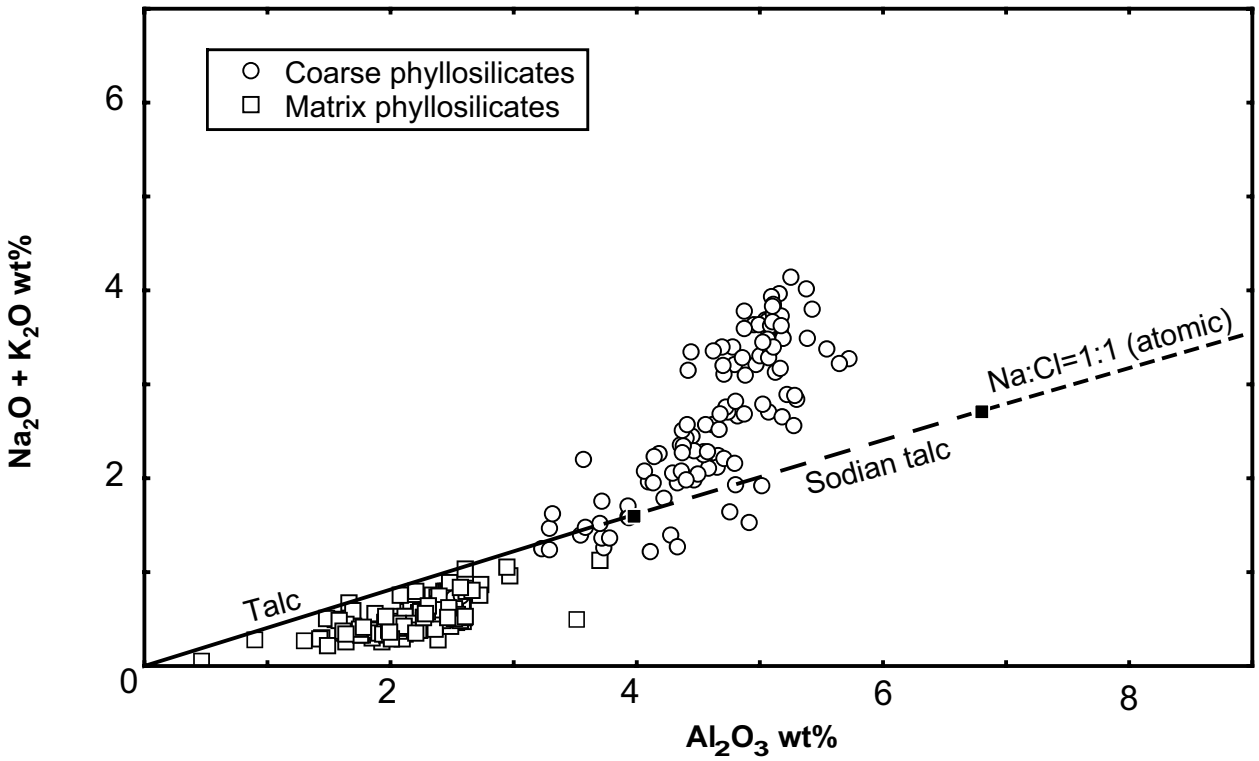

Fig. 3. Chemical compositions of coarse and matrix phyllosilicates in Y-86029 in terms of $Na_2O + K_2O$ versus Al_2O_3. They plot between stoichiometric talc and sodian talc.

Table 2. Microprobe analyses (in wt%) of anhydrous silicates and associated phases in Y-86029.

	Aggregate-1				Aggregate-2	
Species	1	2	3	4	5	6
SiO_2	34.9	59.1	33.6	36.5	39.8	39.9
TiO_2	0.01	0.19	0.27	0.21	0	0.07
Al_2O_3	0.03	0.05	6.89	4.39	0.06	0.05
FeO	39.8	0.76	30.7	34.9	14.6	23.3
MnO	0.29	0.05	0.32	0.35	0.22	0.24
Cr_2O_3	0.30	0.46	0.21	0.11	0.43	0.44
MgO	24.3	39.1	14.9	15.9	45.4	35.4
CaO	0.19	0.54	4.15	3.70	0.03	0.46
Na_2O	0	0	0.96	0.26	0.02	0.07
K_2O	0	0	0.14	0.12	0	0.02
P_2O_5	0	0	0.86	0.85	0.01	0.01
S	0	0	1.44	1.85	0	0
NiO	0.13	0.01	1.30	0.37	0.06	0.07
Total	100	100	95.7	99.4	100	100

1 = Olivine aggregate (average of 10 analyses).
2 = Pyroxene within the olivine aggregate.
3 & 4 = Vein-like inclusion within olivine aggregate.
5 & 6 = Polycrystalline olivine aggregates (average of 15 analyses).

the olivine-rich grains suggest they were once a single isolated crystal later separated by incorporation of the vein. The other large aggregate (Figures 9d and 9e) contains a mosaic of relatively unaltered subhedral to equigranular grains of olivine and minute grains of pyrrhotite and pentlandite (<10 μm). These polycrystalline aggregates have wider olivine compositions (Table 2; $Fo_{84–69}$) and are surrounded by very thin translucent zones (small size precludes accurate microprobe analysis). These translucent zones consist mainly of subhedral, fine-grained ferrous olivine (based on SEM EDXA). Some of the polycrystalline olivine grains have altered to Fe-rich phyllosilicates, which

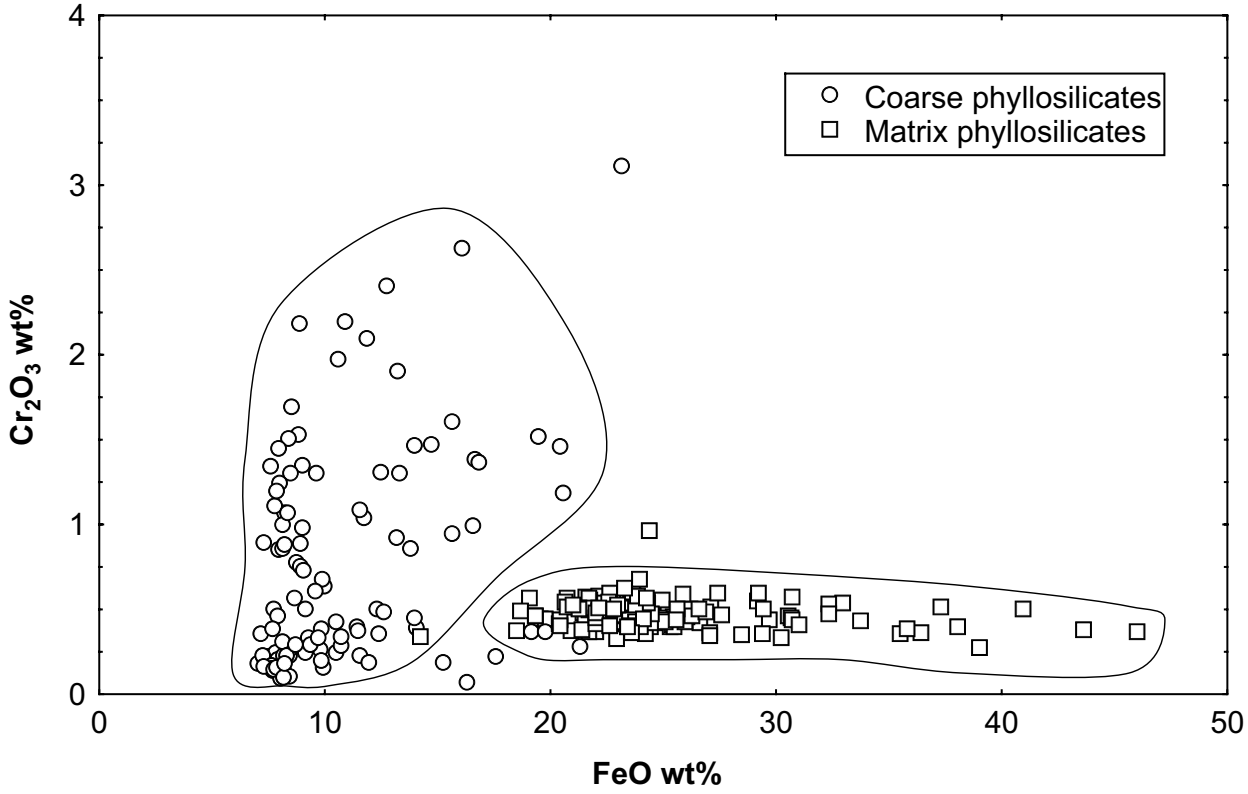

Fig. 4. The Cr_2O_3 contents of phyllosilicates in Y-86029 plotted against FeO (all Fe as FeO). The Cr/Fe ratios of coarse phyllosilicates are lower than matrix phyllosilicates.

show lower analytical totals than matrix or vein phyllosilicates of the previous olivine grain. The tiny sulfide grains are highly abundant and dispersed within these crystals. Slightly larger pyrrhotite clusters are also present.

A compositional profile across the grain shown in Figure 9a displays that the boundary between the aggregate and vein is sharp; the vein is enriched in Al_2O_3, S, CaO, and P_2O_5 and slightly depleted in SiO_2 and FeO relative to the aggregate (Fig. 10). This vein has phyllosilicate compositions (Table 2) with high Al_2O_3 (4.39–6.89 wt%) and FeO (30.70–34.86 wt%) contents and narrow Fe/(Mg + Fe) ratios i.e., 0.38–0.52 (average of 0.44), suggesting homogeneity in composition. The slightly high CaO (2.1–4.9%) and P_2O_5 (0.62–0.86%) contents suggest presence of other finer-grained inclusions of a Ca-P phase, possibly apatite, which is abundant in Y-86029. This vein and surrounding matrix has high analytical totals (97.1–99.5%).

Periclase

Under the light microscope, periclase appears as large brownish clasts, which can be easily confused with coarse-grained phyllosilicates. We have identified two large grains (300–500 μm) and a few other smaller (10–60 μm) grains of periclase within the matrix of Y-86029 (Fig. 11). One of the large grains (Fig. 11a) is sprinkled by minute grains of a Fe-S phase (small size precludes accurate EPMA analysis), while the other is sulfur-poor (Fig. 11b).

Both sulfur-rich and sulfur-poor periclase grains are Fe-bearing and have similar compositions i.e., $Mg_{0.68}Fe_{0.37}Mn_{0.01}O$ and $Mg_{0.68}Fe_{0.30}Mn_{0.02}O$, respectively (Table 3). Their MgO/(MgO + FeO) ratios are also fairly homogenous i.e., 0.53–0.66 for sulfur-poor grains and 0.50–0.65 for sulfur-rich grains. The reason for their analytical totals being slightly low is unclear, but this is probably due to their very fine-grained, porous nature. The slightly higher analytical totals of sulfur-rich than sulfur-poor periclase appear to be due to the fine-grained inclusions of the Fe-S phase in the former.

Magnetite

Magnetite is abundant within Y-86029 in different sizes and essentially all morphologies (framboidal aggregates, spherulites, placquettes, and euhedral crystals) either individually or intergrown (Fig. 12). These magnetite morphologies are characteristic of CI (Jedwab 1971; Kerridge, Mackay, and Boynton 1979) as well as most other carbonaceous chondrites. Minerals intergrown with magnetite include coarse phyllosilicates (Fig. 12c), apatite, and sulfides. Figure 12a shows framboidal aggregates, placquettes, and spherules of magnetite co-existing in an aggregate with a distinct rounded outline. Some of these

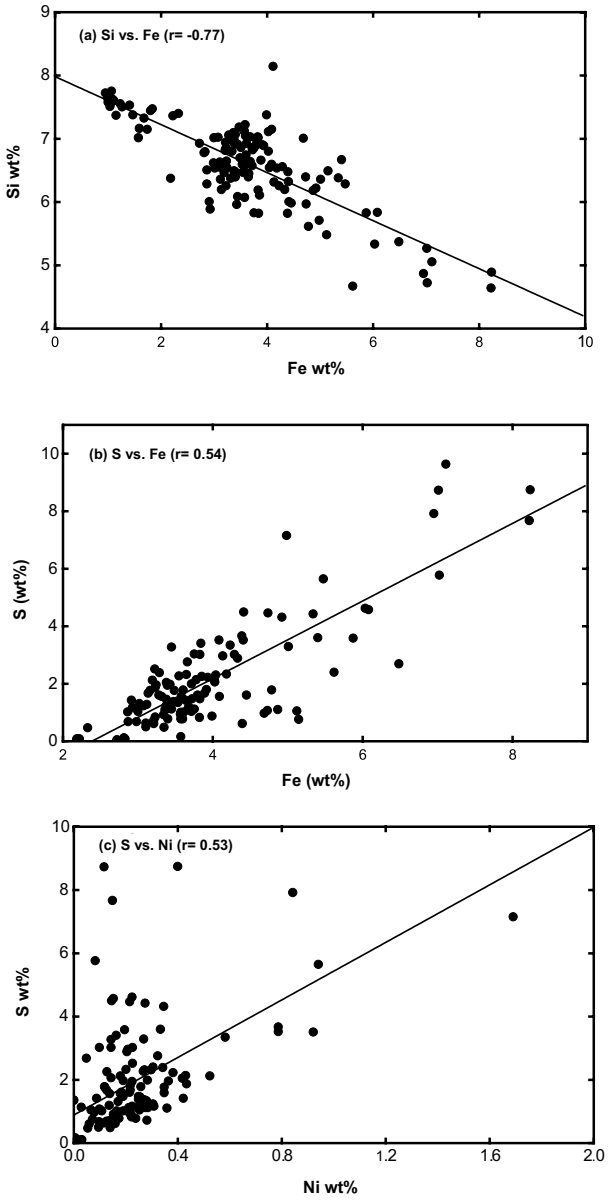

Fig. 5. Distribution of Fe, Ni, S, and Si in the Y-86029 matrix (WDS data). The correlation coefficient defined by the linear regression line and significant at ±0.50 is defined by r. a) Plot of Si versus Fe (r = –0.77); b) Plot of Fe versus S (r = –0.54); c) Plot of S versus Ni (r = –0.53).

magnetite grains with particularly spheroidal types contain inclusions of Fe-sulfides suggesting that they could have resulted from alteration of Fe-sulfide as previously observed in some carbonaceous chondrites (e.g., Tomeoka, Kojima, and Yanai 1989b). Elongated magnetite grains with sulfide inclusions like those in Fig. 12d appear to be heating products of sulfides (see discussion). In general, there is no difference in chemical compositions among the various magnetite textural types, except those within rounded to sub-rounded carbonates, which show high MnO contents (2.5–6 wt%).

Apatite

Apatite ($Ca_{4.9}P_{2.8}O_{12}$) is the only phosphate occurring in Y-86029. It is highly abundant and occurs as large grains (up to 100 μm) within the matrix (e.g., Fig. 12a), often associated with magnetite, carbonate, or coarse-grained phyllosilicates.

Ilmenite

Ilmenite (average composition $Fe_{0.8}Mg_{0.15}Mn_{0.06}TiO_3$) is common within the matrix of Y-86029 as small (20–50 μm) isolated grains. Their (Fe + Mn + Mg)/Ti ratios range from 1.1 to 2.3, suggesting that some of these grains have an Fe oxide (probably hematite) component.

Carbonates

Carbonates are present in Y-86029 as small (10–15 μm) rounded to sub-rounded aggregates (Fig. 13) or individual grains (<25 μm) within the matrix (Figures 14a and 14b). The individual crystals have compositions (Table 3) ranging from magnesite ($Mg_{0.93}Fe_{0.19}CO_3$) to dolomite ($Ca_{0.61}Mg_{1.15}Fe_{0.4}Mn_{0.05}[CO_3]_2$). Both are associated with pyrrhotite (average composition $Fe_{0.82}S$), often rimming magnesite (Fig. 14a). Fine-grained, poorly crystalline Mg-Fe-Mn phases occur adjacent to these crystals.

The rounded to sub-rounded carbonate aggregates (Fig. 13) occur within a void. They occur as 'shells' of ankerite ($Ca_{1.03}Fe_{1.12}Mn_{0.15}[CO_3]_2$), and some siderite ($Fe_{1.02}Mn_{0.10}CO_3$), enclosing magnetite. Spaces between these aggregates are filled with dolomite ($Ca_{0.97}Mg_{0.98}Fe_{0.05}[CO_3]_2$) and poorly-crystalline Ca phases. Mixtures of carbonate and sulfides also occur within or on the peripheries of these carbonates (Figures 13b and 13c; Table 3). Microprobe analyses shows that these carbonates plot between the Ca-carbonate and siderite (Fig. 15) on the Ca-Mg-Fe ternary diagram. The Fe and Mn exhibit no systematic relationship (Fig. 16), neither positively correlating with nor substituting for each other. These carbonates have uniform, fine-grained texture and compositional patterns as depicted in the element compositional maps (Fig. 17).

Sulfides

Iron sulfides, mostly pyrrhotite, and a few grains of pentlandite are abundant in Y-86029. This abundance is higher than that in non-Antarctic CI chondrites (Bullock et al. 2002). Pyrrhotite occurs as large (10–60 μm) euhedral, anhedral, and lath-like grains and also as small grains (sub-micron scale) widely dispersed in the matrix. These pyrrhotites contain variable amounts of Ni (0.2–4.5 wt% NiO). Pentlandite grains are rare and relatively small (<5 μm) and occur mainly within the anhydrous mineral grains. Most of these sulfides are relatively fresh and exhibit little evidence of weathering.

Table 3. Microprobe analyses of selected carbonates and periclase in Y-86029.

Species	Matrix Carbonate		Rounded carbonates			Periclase	
	Magnesite	Dolomite	Ankerite	Dolomite	S-rich[a]	1	2
SiO_2	0.73	0.81	0.58	0.53	0.45	0.27	0.33
TiO_2	0	0	0	0.01	0.02	0.03	0
Al_2O_3	0.20	0.03	0.20	0.03	0	0	0.01
FeO	14.3	12.9	30.9	3.88	39.8	41.3	38.9
MnO	2.20	3.81	3.16	1.11	3.41	1.49	2.89
Cr_2O_3	0.01	0.01	0	0	0	0.01	0.03
MgO	37.6	21.8	10.5	20.5	16.0	51.5	49.8
CaO	4.01	23.9	20.5	30.1	23.8	0.05	0.06
Na_2O	0.08	0.09	0.07	0.36	0	0.04	0.04
K_2O	0.03	0.02	0.01	0.03	0.04	0	0
P_2O_5	0.05	0.21	0.12	0.08	0.23	0	0
S	0.31	0.50	0.87	0.80	6.89	0.91	0.10
NiO	0.56	0	0.07	0.21	0	0.05	0
Total	60.1	63.6	66.9	57.7	90.6	95.6	92.1

[a]Mixed sulfide-carbonate phase.
1 = sulfur-rich.
2 = sulfur-poor.

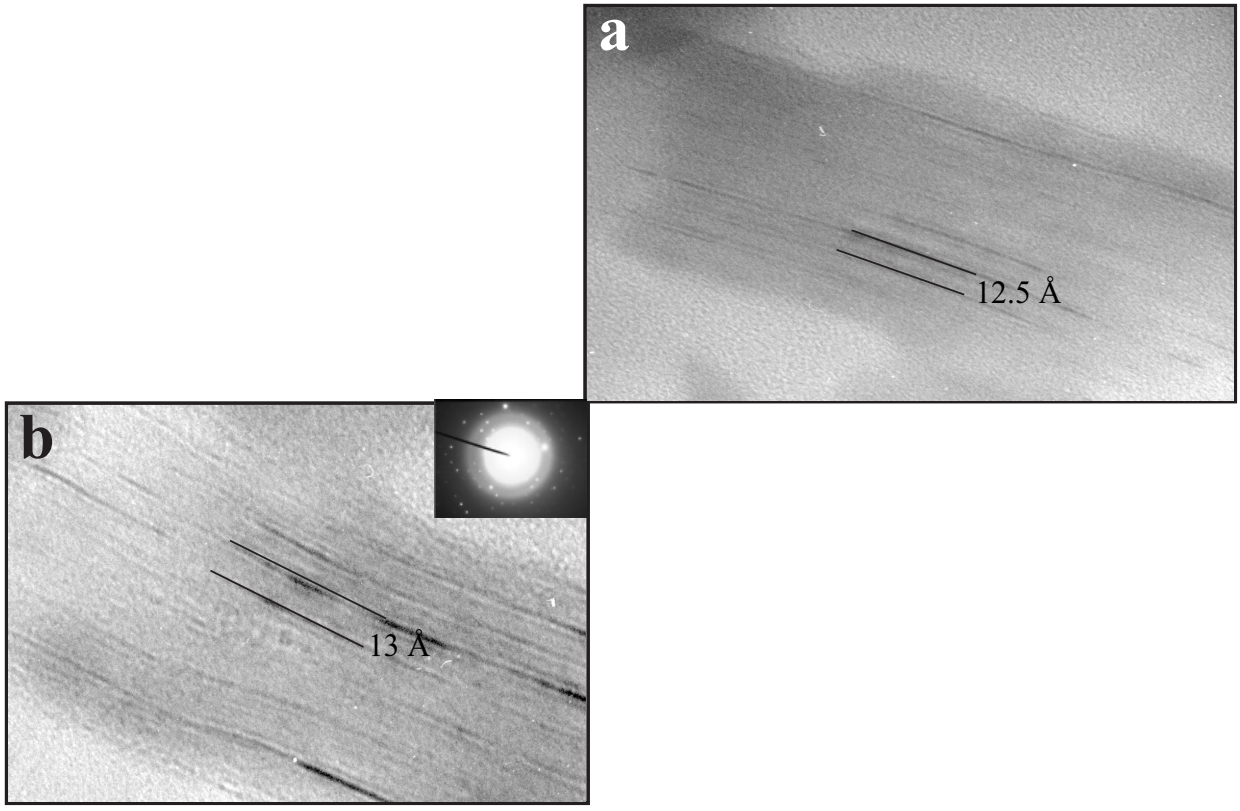

Fig. 6. Electron micrographs of matrix textures of Y-86029. Thick 'patchy' or platy phyllosilicate-like crystals (a and b) are distributed within the matrix with d-spacings between 9 Å and 13 Å. A typical diffraction pattern is shown in Fig. 6b.

TRACE ELEMENT CHEMISTRY

In Table 4, we list data for the 14 trace elements in the RNAA suite in Y-86029 compared with those in Y-82162 (Paul and Lipschutz 1989, 1990) and Orgueil CI chondrites (cf., Anders and Grevesse 1989, as updated by Friedrich, Wang, and Lipschutz 2002). We order these elements by increasing degree and ease of their volatization and loss during extended (1 week) heating of primitive meteorites, primarily Murchison and Allende (Ikramuddin and Lipschutz 1975; Matza and Lipschutz 1977; Bart, Ikramuddin, and Lipschutz 1980; Ngo and Lipschutz 1980),

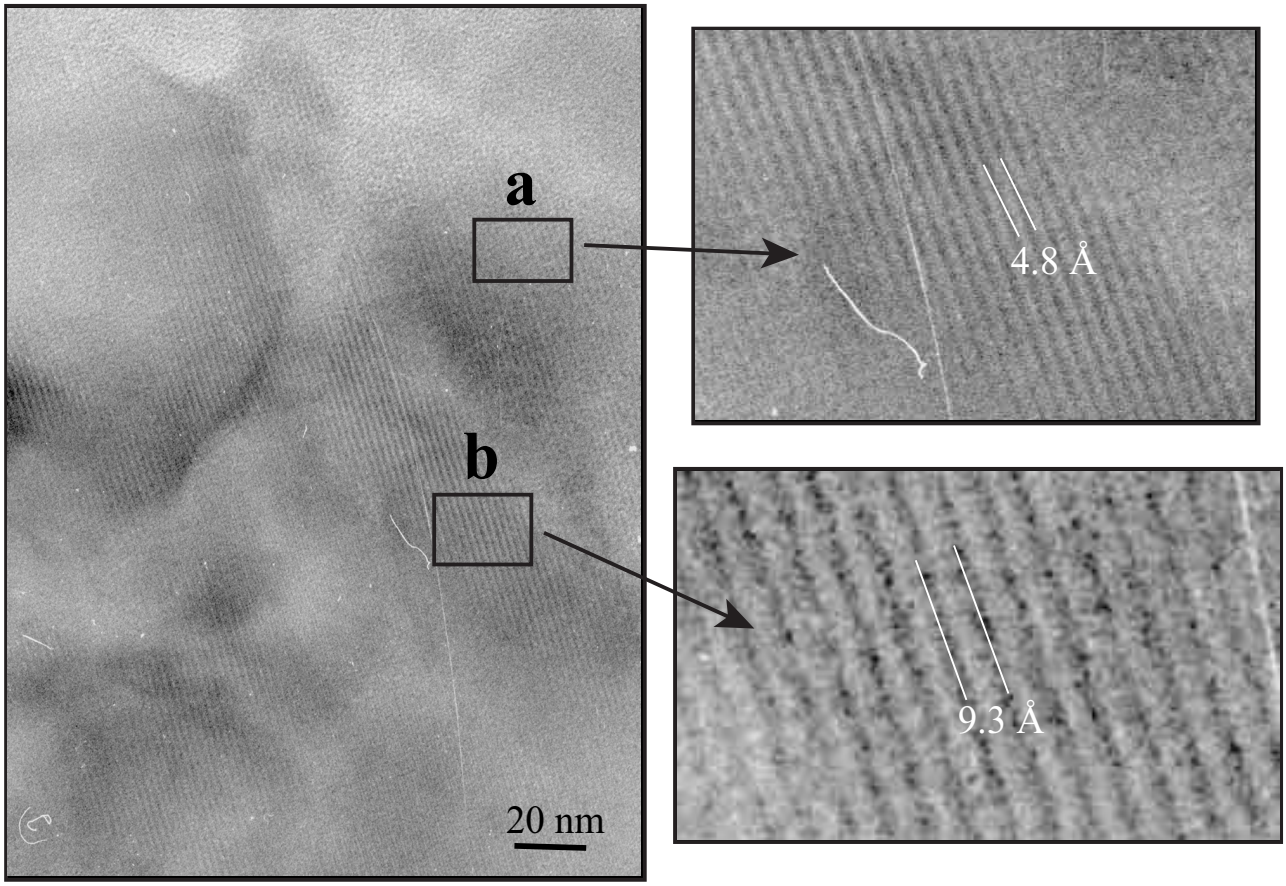

Fig. 7. High-resolution electron micrograph of better-developed crystals in Y-86029. The d-spacings are not typical of phyllosilicates. Lattice d-spacings of about 9–10 Å (b) are predominant, which are presumably 'intermediate phases' during the transformation of phyllosilicates to anhydrous silicates. Lattice d-spacing of 4.8 Å corresponds to d_{100} of olivine.

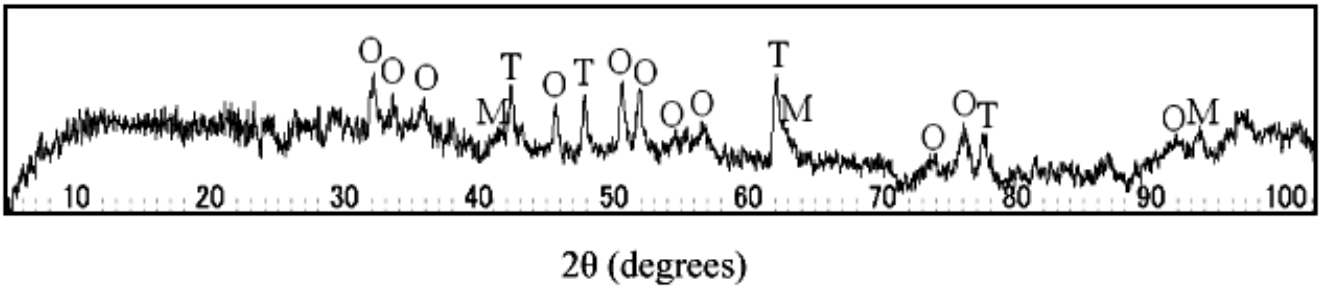

Fig. 8. X-ray powder diffraction pattern (Cr, Kα) of matrix of Y-86029. O, M, and T indicate olivine, magnetite, and troilite reflections respectively.

under ambient atmospheric conditions (initially 10^{-5} atm H_2) reasonable for primitive solar system objects. Prior studies have shown that these data constitute a contextual format for identifying carbonaceous chondrites thermally metamorphosed in their parent asteroids (Paul and Lipschutz 1989, 1990; Xiao and Lipschutz 1992; Hiroi et al. 1993, 1994, 1996; Wang et al. 1998; Lipschutz, Zolensky, and Bell 1999; Friedrich, Wang, and Lipschutz 2002). We should note that in the absence of published data for an artificially heated CI chondrite, we explicitly assume that the extent of mobile trace element loss from such a sample is that observed for Murchison. Unpublished data for Ivuna (Wang, Zolensky, and Lipschutz 2000) confirm that the open system heating data for CI chondrites is indeed compatible with that of Murchison.

Two of the 3 most refractory elements (Co → Sb) in Y-86029 accord well with data for Y-82162 and Orgueil (Table 4). The high Au level in Y-86029 may signal the presence of

Table 4. Trace element data obtained by RNAA for Y-86029 compared with prior results for Y-82162 and Orgueil CI chondrites.

Element[a]	Y-86029	Y-82162[b]	Orgueil[c]†
Co (ppm)	516	490	507
Au (ppb)	357	102	145
Sb (ppb)	120	140	160
Ga (ppb)	12.1	13.2	10.1
Rb (ppm)	1.69	3.2	2.30
Cs (ppb)	201	211	186
Se (ppm)	24.9	27.8	21.4
Ag (ppb)	294	291	197
Te (ppm)	2.44	3.12	2.27
Zn (ppm)	340	364	311
In (ppb)	22.2	39	77.8
Bi (ppb)	23.4	23.4	111
Tl (ppb)	12.9	3.37	143
Cd (ppb)	115	1.4	680

[a]Elements ordered by increasing degree of loss from Murchison artificially heated at 600–700°C (Matza and Lipschutz 1977).
[b]Paul and Lipschutz (1989).
[c]Anders and Grevesse (1989) as updated by references in Friedrich, Wang, and Lipschutz (2002).

a small Fe-Ni metal grain(s); such heterogeneity is not unprecedented in a 50 mg sample.

Contents of the next 7 elements (Ga → Zn) are higher in Y-86029 than in Orgueil but are not, on average, as high as those in Y-82162. In discussing the Y-82162 data, Paul and Lipschutz (1989, 1990) suggested that the mean Y-82162/Orgueil ratio for the five most mobile of these elements (Cs → Zn), 1.36 ± 0.18 (Table 5), reflects metamorphic loss of more abundant volatile species—organics, CO_2, and H_2O—in their parent object and the absence of subsequent rehydration of Y-82162. We attribute the lower, nonetheless elevated, Y-86029/Orgueil ratio, 1.20 ± 0.19 (Table 5), to the same cause.

We take as a working hypothesis that the difference between the Orgueil-normalized ratios signals that Y-86029 was thermally metamorphosed under less severe conditions than those affecting Y-82162. The most mobile trace elements support this. Contents of the 4 most mobile trace elements, In → Cd, in Y-86029 and Y-82162 are undoubtedly depleted relative to Orgueil. Those of Tl and Cd are even lower in Y-82162 than in Y-86029 (Table 4).

To place the Y-82162 and Y-86029 data on absolute basis, we show (Figure 18) CI-normalized data for the 9 most mobile elements (Cs → Cd) in these two CI-like chondrites and Murchison (CM2) artificially heated at 500–700ºC (Matza and Lipschutz 1977). The data for Y-82162 accord with those of Murchison heated at 600–700ºC, while the Y-86029 results suggest lower temperatures of 500–600ºC. Lipschutz, Zolensky, and Bell (1999) found the temperatures estimated from the RNAA data generally accord with temperatures indicated by petrographic and mineralogical alteration in carbonaceous chondrites.

OXYGEN ISOTOPES

Whole-rock sample of Y-86029 was analyzed for oxygen isotopes by the methods of Clayton and Mayeda (1963, 1983). The isotopic compositions are reported as ‰ deviations from the SMOW (standard mean ocean water) standard for both $^{18}O/^{16}O$ and $^{17}O/^{16}O$ ratios. The values for Y-86029 i.e., $\delta^{18}O = +21.89$ and $\delta^{17}O = +11.59$ (Mayeda and Clayton, personal communication 2002), are very similar to those of Y-82162 i.e., $\delta^{18}O = +21.56$ and $\delta^{17}O = +11.59$ (Clayton and Mayeda 1999). This falls above the CI chondrite field (represented by Alais, Ivuna, and Orgueil) and much closer to those of Y-86720, Y-86789, and B-7904 (Fig. 19).

Table 5. Atomic abundances (Cl-normalized) for thermally mobile trace elements in Y-86029 compared with prior data for CI and CM/C2 chondrites that lost ≤2 elements during thermal metamorphism in their parent bodies.

		CI1-normalized atomic abundances			
Meteorite	Type	$\bar{x} \pm \sigma$[a]	Elements (No.)	Cd	ref.[b]
PCA 91008	C2	0.46 ± 0.13	Cs → Bi (7)	0.0092	(2)[c]
Y-86029	CI1	1.20 ± 0.19	Cs → Zn (5)	0.168	(1)[d]
B-7904	CM	0.57 ± 0.08	Cs → Zn (5)	0.0022	(3)[e]
Y-82162	CI1	1.36 ± 0.18	Cs → Zn (5)	≤0.0021	(3)[f]
Y-86720	CM	0.65 ± 0.16	Cs → Te (4)	0.0010	(3)[g]
Y-86789	CM2	0.69 ± 0.08	Cs → Te (4)	0.0031	(2)[h]

[a]Mean ± σ depletion factors for elements in next column unaffected by thermal metamorphism.
[b]References: (1) This work; (2) Wang and Lipschutz (1998); (3) Paul and Lipschutz (1989).
[c]Also Tl = 0.16.
[d]Also In = .029; Bi = 0.20; Tl = 0.091.
[e]Also In = 0.36; Bi = 0.13; Tl = 0.032
[f]Also In = 0.51; Bi = 0.21; Tl = 0.024.
[g]Also Zn = 0.076; In = 0.16; Bi = 0.028; Tl = 0.024.
[h]Also Zn = 0.082; In = 0.12; Bi = 0.080; Tl = 0.033

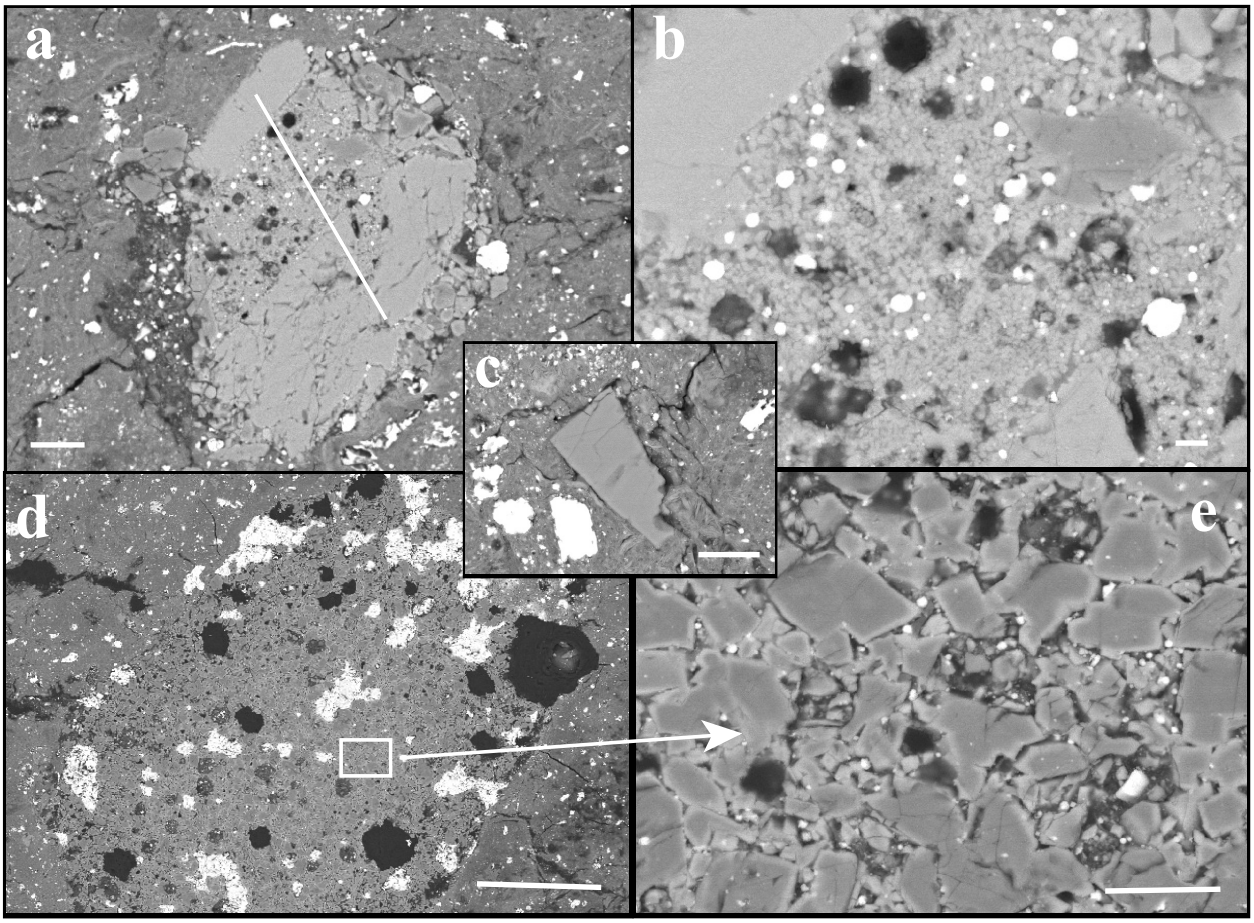

Fig. 9. BSE images of anhydrous silicates in Y-86029: a) Olivine aggregate (Ol) cross-cut by a vein (Vn). Line A-B is the compositional profile shown in Fig. 4; b) A close up of the vein in (a) showing its porous nature and tiny grains of pyrrhotite (Py) and pentlandite (Pn); c) An isolated fayalitic olivine (Fo_{49}) grain within the matrix; d) Olivine aggregate (Ol) consisting of polycrystalline grains and pyrrhotite clusters (Py); e) A close up of the polycrystalline olivine crystals (Ol) showing minute grains of Fe-S phase (probably pyrrhotite) interspersed between crystals. These grains have thin outer translucent zones. Scale bars = 10 μm.

DISCUSSION

Aqueous Alteration and Thermal Metamorphism

Petrographic characteristics of Y-86029 are CI-like i.e., Y-86029 lacks chondrules and consists mainly of matrix as a result of extensive aqueous alteration. A general model for alteration of CI chondrites involves progressive leaching of Ca, Mn, and Na from fine-grained matrix and oxidation of S (from sulfides) to produce carbonates and sulfates. However, recent studies suggest that sulfates in CI chondrites are largely or entirely terrestrial in origin (Gounelle and Zolensky 2001). Oxidation of ferric iron results in formation of magnetite and ferrihydrite (e.g., Richardson 1981; Brearley and Prinz 1992; Zolensky, Barrett, and Browning 1993). This process effectively fractionates Fe from the fine-grained phyllosilicate portion of the matrix into magnetite and Mg-rich compositions (Brearley 1997).

Based on depletion of Ca and Mn in the matrices of CI chondrites, Brearley and Prinz (1992) suggested that there was significant variability in the degree of leaching and late stage oxidation experienced by the different CI chondrites. Based on fe#, Y-86029 represents an intermediate stage in the alteration sequence together with Alais and Ivuna (fe# = 0.30) as compared with the most altered Orgueil (fe# = 0.15). Elemental correlations suggest that the Y-86029 phyllosilicates are fairly homogeneous at the millimeter scale as observed in most CI chondrites (e.g., Orgueil or Ivuna). Variations in Ni contents may be due to the presence of sub-micron pentlandite grains. Tomeoka and Buseck (1988) showed evidence that coarse phyllosilicates in Orgueil were attacked by Fe-rich aqueous solutions and were decomposed to fine phyllosilicates resulting in precipitation of ferrihydrite in the process. They further explained that the ferrihydrite resulted from alteration of magnetite and Fe-Ni sulfides as well as precipitation from Fe-rich solutions. We agree with their observation that the presence of large clusters of coarse phyllosilicates in Y-82162 suggests the absence of a late stage

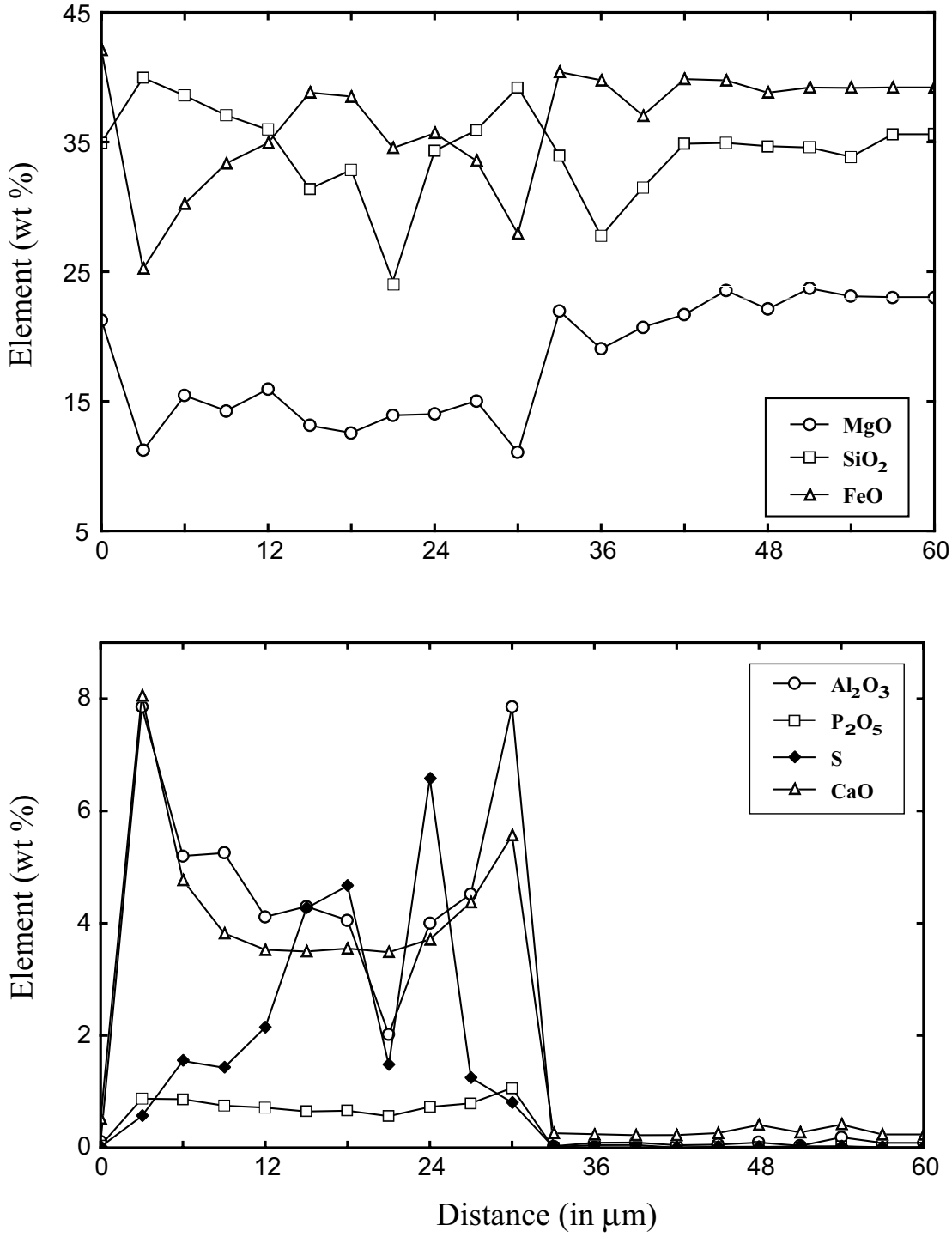

Fig. 10. Compositional profiles across line A-B (starting from A) in olivine aggregate of Fig. 9a showing the distribution of MgO, SiO_2, FeO, Al_2O_3, P_2O_5, S, and CaO. The boundaries between the vein and aggregate occur at 3 μm and 33 μm respectively.

aqueous alteration phase, but it is important to emphasize that no studies to date have confirmed the extraterrestrial origin of ferrihydrite. The coarse phyllosilicates in Y-86029 have high Na_2O contents (1.57–4.53 wt%) in contrast to matrix of Orgueil, Alais, and Ivuna, which are strongly depleted in Na relative to the bulk meteorite (McSween and Richardson 1977), and probably resulting from leaching during intense aqueous alteration.

The coarse and matrix phyllosilicates in Y-86029 record a thermal metamorphic event. They show dehydration to olivine (apparent in the high analytical totals (88.3–97.8; average 91.7 wt%), microscale (TEM), and XRD

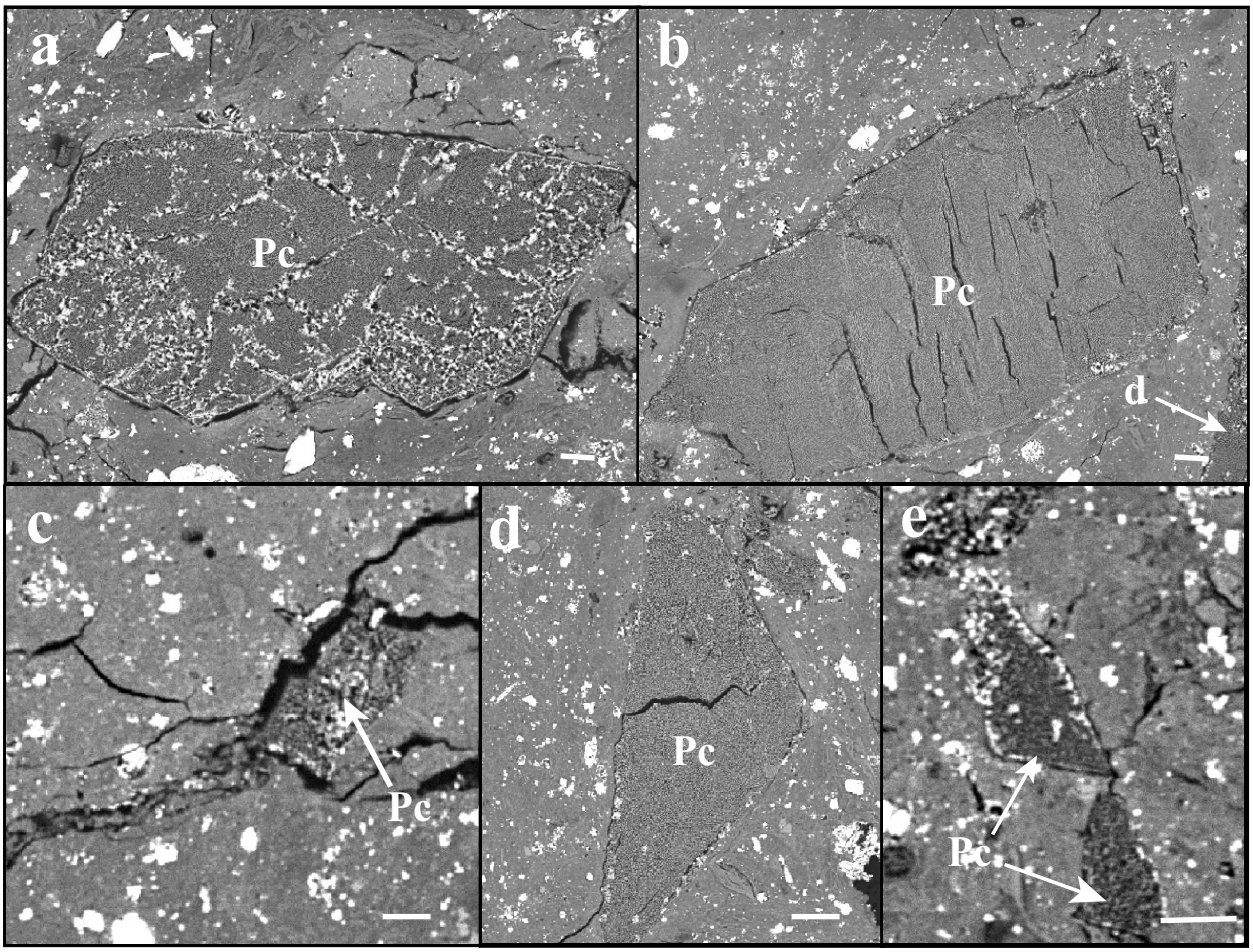

Fig. 11. Distribution of periclase in Y-86029: a) large periclase (Pc) grain with minute grains of FeS phase; b) large sulfide-free periclase grain (Pc); c) periclase (Pc) occurring within a fracture zone; d) smaller sulfide-free periclase (Pc) grain adjacent to the larger grain in (b); e) smaller periclase grains (Pc) with sulfide inclusions. Scale bars = 10 μm.

observations. This material exhibits highly disordered and defect structures with lattice fringes between 9 Å and 13 Å (9 Å to 10 Å is predominant). Small areas with 4.7 to 4.8 Å lattice fringes correspond to d_{100} basal spacings of olivine. The crystallization of olivine from residual serpentine as a result of thermal decomposition is also apparent in XRD reflections.

Minerals with highly disordered and defect structures are normally derived by transformation of serpentine- or saponite-type phyllosilicates to olivine (Brindley and Zussman 1957; Ball and Taylor 1963; Brindley and Hayashi 1965; Akai 1988). These 'intermediate' phases consist of newly formed olivine, residual desiccated phyllosilicate and their mixtures. The data do not accord with the opposite transition i.e., from olivine to phyllosilicate because the lattice features do not fit well with olivine grains but with original phyllosilicates. In addition, hydrothermal experiments to derive serpentine from olivine (Brindley and Zussman 1957; Brindley and Hayashi 1965) do not show such transitional states. The patches and defects may correspond to a distribution of 'donor and acceptor regions' in the phase transformation as proposed by Ball and Taylor (1963). These phases have previously been observed in only one thermally metamorphosed meteorite i.e., Y-793321 (Akai 1988). However, more detailed studies are necessary to determine their crystallographic and structural properties. Transformation of serpentine to forsterite is known to commence in the range between 500 and 600°C (Brindley and Brown 1984), which is within the range of heating temperatures experienced by Y-86029 based on RNAA data.

This level of thermal metamorphism is also apparent in the compositions of the carbonates. Thermally decomposed Ca-Mg-Fe-Mn carbonates and associated poorly crystalline Fe-Mn oxides are abundant in Y-86029 rather than calcite or dolomite as is the case in most CI chondrites. Periclase also appears to be a heating product of initially Mg-rich carbonates (discussed in the following section). The elongate magnetite crystals with sulfide inclusions observed in Y-86029 and Y-82162 (Zolensky, Barrett, and Prinz 1989a) could also be heating products of sulfides.

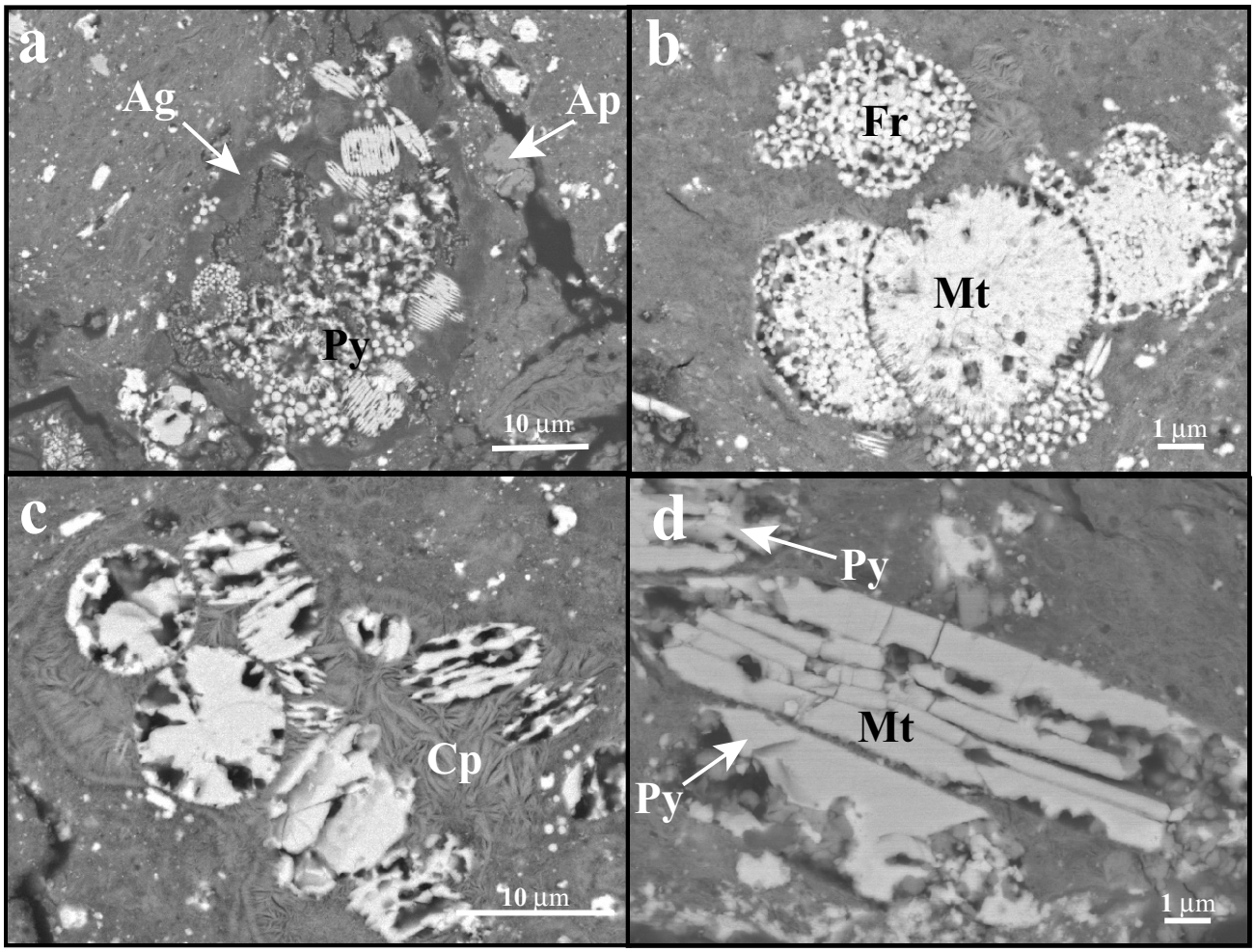

Fig. 12. Distribution of magnetite in Y-86029: a) magnetite plaquettes, framboids, and spherulites occurring within an altered undetermined aggregate (Ag). Pyrrhotite (Py) occurs within these magnetite grains. Notice the apatite (Ap) grain within the matrix; b) magnetite spherulite (Mt) and framboids (Fr); c) magnetite spherulites (Mt) enclosed within coarse phyllosilicates (Cp); d) elongate magnetite grain (Mt) with small pyrrhotite clusters (Py) within or adjacent to the grain.

The high $\delta^{18}O$ and $\delta^{17}O$ isotopic ratios in Y-86029 and Y-82162 can also be attributed to heating. The process that governs the mass dependant fractionation associated with water loss is, however, poorly understood at this stage, although the direction of fractionation is the same, i.e., preferential loss of isotopically light water, is accompanied by concomitant heavy isotope enrichment in the solid residue (Mayeda and Clayton 1999).

Y-86029 joins a growing list of Antarctic carbonaceous chondrites that experienced heating events in asteroidal settings (Paul and Lipschutz 1989; Wang et al. 1998; Lipschutz, Zolensky, and Bell 1999; Tonui et al. 2002b). The absence of thermally metamorphosed carbonaceous chondrite falls remains noteworthy. The significance of petrologic, chemical, and isotopic differences between non-Antarctic and Antarctic meteorites has long been emphasized (e.g., Takeda et al. 1983; Dennison, Lingner, and Lipschutz 1986; McGarvie et al. 1987), suggesting differences in meteoroid flux between contemporary falls and substantially older Antarctic meteorites, implying distinct genetic histories. Spectral reflectance data in the ultraviolet (UV), visible and near infrared (IR) for the thermally metamorphosed meteorites reveal that they resemble those of the surfaces of a number of C-, G-, B-, and F- asteroids. Thus Hiroi et al. (1993, 1994, 1996) suggested that the surfaces of these asteroids consist of carbonaceous chondrite-like material metamorphosed over a range of temperatures in the parent bodies' interiors, then excavated by impacts and re-deposited on their exteriors.

The source of thermal metamorphism in carbonaceous chondrites is still uncertain. It is also uncertain as to whether this metamorphism occurred in short-lived phases or was a terminal event occurring after all other post-accretionary processes. Certainly, petrographic studies of heated carbonaceous chondrites to date (e.g., Tonui et al. 2002b) show that it was a dominant late stage event occurring after aqueous alteration. However, the occurrence of ephemeral

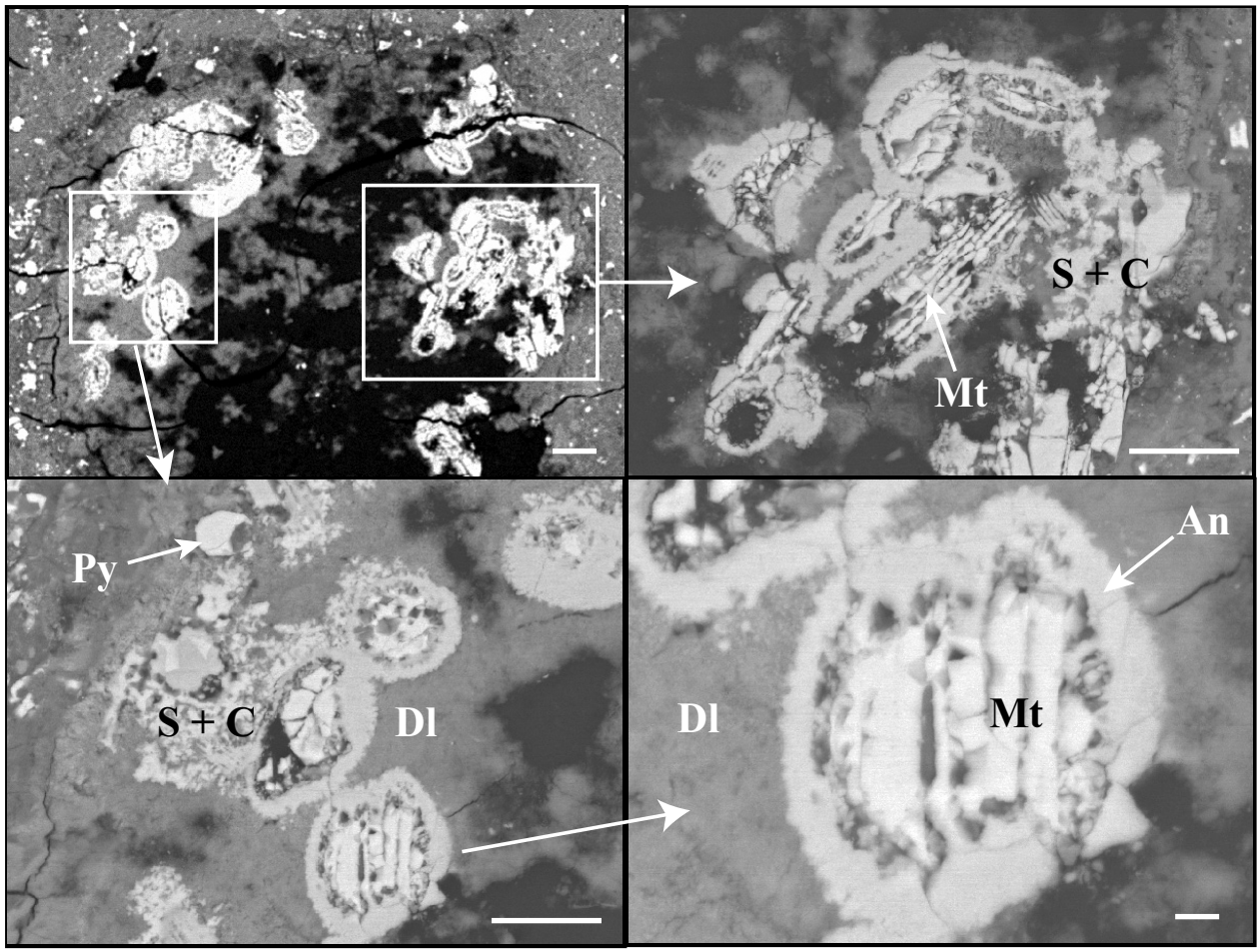

Fig. 13. Distribution of rounded to sub-rounded carbonates in Y-86029: a) occurrence of the carbonates within a void in Y-86029; b) close up view of region in (a) showing elongate magnetite crystals (Mt) enclosed within the carbonate. Carbonate enclosing the magnetite shown in the figure is fragmented. Mixtures of sulfide and carbonate (S + C) occur adjacent to these carbonates; c) close up view of region in (a) showing the rounded to sub-rounded carbonates, mixtures of sulfide and carbonate (S + C), and pyrrhotite (Py). Dolomite (Dl) occurs in interstices; d) a close up of a rounded to sub-rounded carbonate consisting of magnetite (Mt) enclosed within ankerite (An) and dolomite (Dl) in interstices. Scale bars: d = 1 μm; others = 10 μm.

heating events cannot be easily established since their effects would be obscured by late-stage retrograde aqueous alteration. Therefore, it is difficult to place precise constraints on the timing of these heating events, which could give clues as to the possible thermal decomposition temperatures of most of the mineral phases. For the purposes of this paper, we envisage thermal metamorphism as one heating episode, which melted ice and caused aqueous alteration in initial stages, and continued on to later dehydrate and recrystallize the secondary minerals.

Combining thermally mobile trace elements as markers of metamorphic episodes with petrographic observations permits Y-86029 to be ranked with other carbonaceous chondrites (Table 5). The temperature range for primitive carbonaceous chondrites that lost ≥2 elements during thermal metamorphism in their parent bodies is: 500ºC <PCA 91008 (C2) <Y-86029 (CI) <B-7904 (CM2) ~Y-82162 (CI1) <Y-86720/Y-86789 (CM2) ≤700ºC.

Unusual Textures of Y-86029

Anhydrous Silicates

Two large olivine aggregates are present in Y-86029; one with a vein with phyllosilicate composition and the other with polycrystalline aggregates of olivine with abundant minute blebs of pentlandite and pyrrhotite. Parallel orientation, optical continuity, and sharp boundaries between the first olivine-rich grain and the vein suggest that the olivine grains were once a single isolated crystal later separated by emplacement of the vein. This vein is as heated as the adjacent matrix.

The polycrystalline olivine grains are well preserved and show minimal aqueous alteration. The textures of this grain and abundance of minute blebs of sulfides suggest it is probably not a remnant of a chondrule. The abundance of minute sulfide grains suggests some recrystallization reaction from a melt. These features are typical of shock-

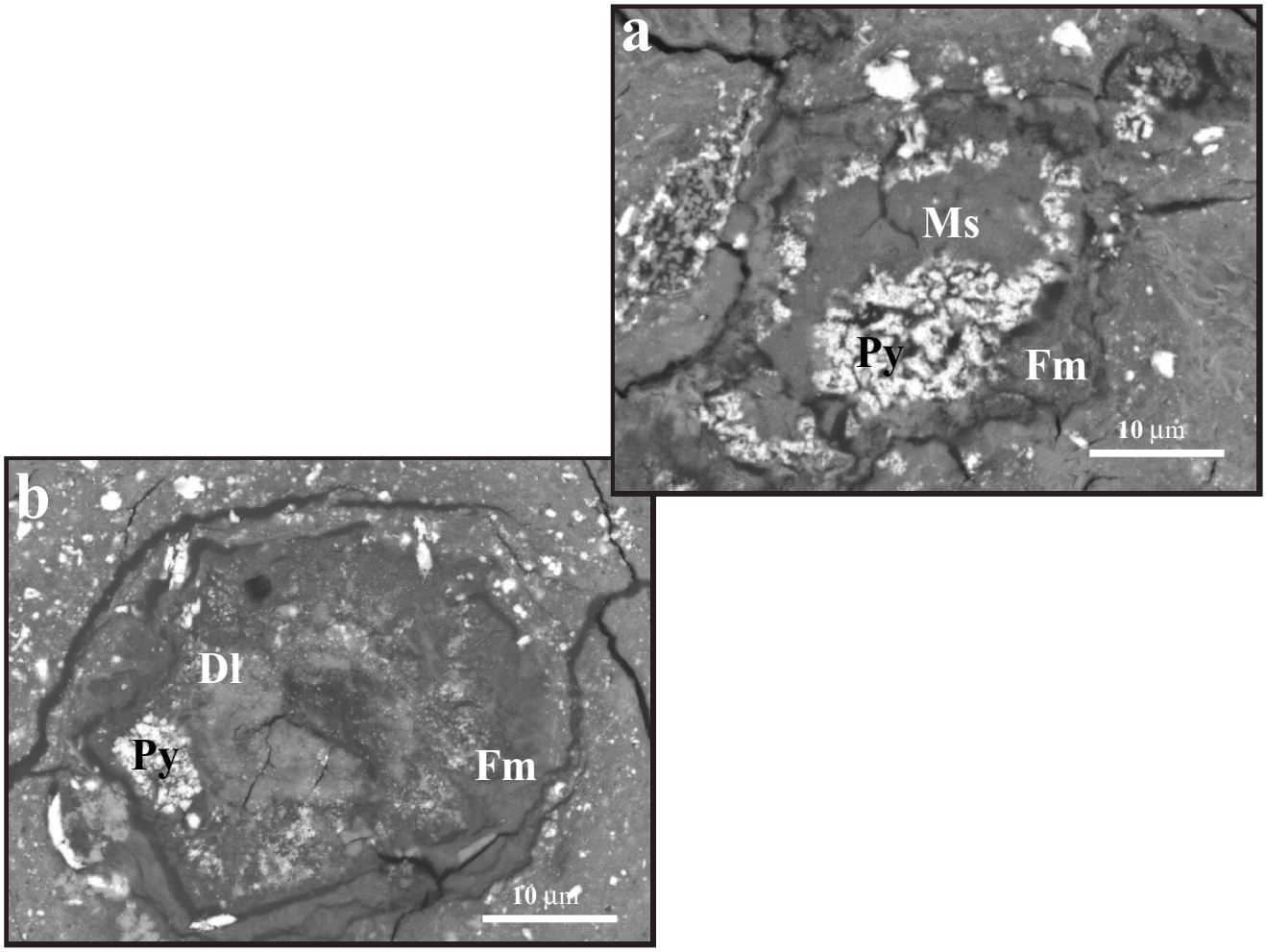

Fig. 14. Distribution of carbonates within matrix of Y-86029: a) magnesite (Ms) rimmed by pyrrhotite (Py) and poorly crystalline Fe-Mn phases (Fm); b) dolomite (Dl) and pyrrhotite (Py) enclosed within poorly crystalline Fe-Mn phases (Fm).

induced intragranular microfractures in olivine associated with low to medium pressure (~45 GPa) impacts and thermally activated processes such as annealing, oxidation, and recrystallization (Bauer 1979; Dodd and Jarosewich 1979; Ashworth 1985). The total melting of olivine must have occurred within regions of the same sample, the resulting melt mixing instantaneously with coexisting, simultaneously shock-melted sulfide grains. The sulfides were probably incorporated into fractures in olivine in a process frequently referred to as 'shock blackening' (Stöffler, Keil, and Scott 1991; Van der Brogert, Schultz, and Spray 2001).

The presence of recrystallization in naturally shocked olivines, however, need not be indicative of high shock loading. Shocked but unannealed olivine can experience recrystallization at rather low temperatures (~400ºC) especially if there is high concentration of lattice defects, which serve as nucleation sites (Reimold and Stöffler 1978). This may simply reflect a later, low-temperature thermal event(s) following weak or moderate shock. The presence of such multiple events, however, is difficult to justify petrographically.

Shock features in CI chondrites have not been described, perhaps because they were never shocked much to begin with or because shocked materials were fragmented and never survived as meteorite-sized objects. It is also possible that shock effects were later erased by subsequent aqueous alteration. There is no additional evidence for shock in any other mineral phases in Y-86029 and hence we cannot conclude that it affected entire rock based on one isolated anhydrous grain. Furthermore, these olivine aggregates should not have survived the extensive aqueous alteration evident in this meteorite. We therefore conclude that these aggregates were mechanically mixed from another environment into the matrix after aqueous alteration was completed. They were possibly derived from elsewhere in the Y-86029 parent asteroid or from fragments that were incorporated into Y-86029 from another asteroid (probably an ordinary chondrite) during an era of asteroid erosion rather than accretion.

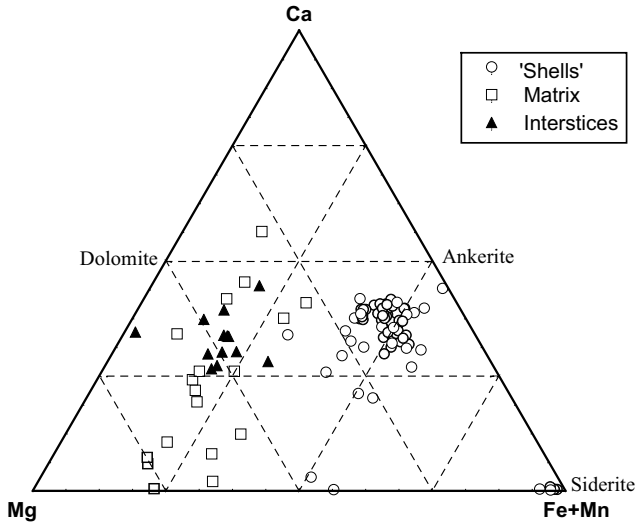

Fig. 15. Composition of carbonates in Y-86029 (WDS data), plotted onto a Ca-Mg-Fe atom% ternary diagram. 'Shells' refer to the rounded to sub-rounded carbonates enclosing magnetite.

Rounded to Sub-Rounded Carbonates

Carbonates in CI chondrites occur mainly as isolated grains of calcite and dolomite and have been interpreted as having formed by low temperature hydrous alteration in asteroidal environments (DuFresne and Anders 1962; Nagy and Andersen 1964; Fredriksson et al. 1980; Fredriksson and Kerridge 1988). The rounded to sub-rounded carbonate aggregates in Y-86029 have not been observed in other carbonaceous chondrites. We referred to these carbonates as being 'globular' in an earlier publication (Tonui, Zolensky, and Lipschutz 2002a), but this term is rather broadly defined, and hence, we now consider it as inappropriate. We have also confirmed on further petrological examination that the composition of these carbonates do not reflect any core to rim sequence or zoning patterns as reported therein.

The rounded to sub-rounded carbonates of Y-86029 are small (10–15 μm) and occur in a void within the matrix. They consist of magnetite enclosed within ankerite with interstices filled with dolomite and poorly crystalline Ca phases. The outlines of these carbonates are reminiscent of the carbonates in Martian meteorite ALH 84001 (e.g., Golden et al. 2001) although the magnetite and enclosing carbonate in Y-86029 show sharp contacts and do not show distinct zoning. Curiously, the dolomite filling the spaces between the carbonates shows little thermal decomposition as compared to the ankerite or the other carbonates within the matrix, implying that it was deposited after the peak heating phase or that the dolomite is more stable at high temperatures.

The origin of these unusual carbonates is unclear but we can postulate a number of explanations based on existing thermodynamic models. The equilibrium solution composition models for carbonates between 25 and 150ºC (Woods and Garrels 1992) is within the compositional ranges of these carbonate phases in Y-86029. For example, magnesite precipitation at 150 and 25°C requires high a_{Mg}^{2+}/a_{Ca}^{2+} (a = activity), while siderite and ankerite precipitation require even higher a_{Fe}^{2+}/a_{Ca}^{2+}. This model suggests that the precipitation of siderite or ankerite occurs when the $a_{Ca}^{2+} >> a_{Fe}^{2+}$.

When this model is applied to Y-86029, it is envisaged that the carbonates that form first from equimolar Ca-Mg-Fe-CO_2 solutions at 150ºC have compositions near the siderite end member. As Fe is removed from solution by the precipitating siderite, the activities of Mg and Ca become predominant, resulting in Ca and Mg enrichment at the outer regions. The Mg activity may not be high enough for formation of magnesite. This might alternatively explain the presence of dolomite in interstices, although later deposition as explained earlier seems more plausible. This model should, however, be treated with caution since it assumes non-equilibrium, closed system conditions with changing solution compositions resulting from fractionation during precipitation, which is not necessarily satisfied in asteroidal environments. Valley et al. (1997) reported that low-temperature carbonate minerals commonly form in apparent violation of equilibrium thermodynamics and the kinetic process that causes the apparent fractionation is not well understood.

It is unclear why some of the carbonates in Y-86029 did not completely decompose or were not transformed to the oxides e.g., periclase (next discussion). It is possible that heating was not uniform in different regions of the meteorite or in the case of dolomite deposited after the peak heating temperatures. A more plausible explanation lies in the decomposition temperatures (T_d) for carbonates of Mg, Ca, and Fe at varying CO_2 total pressures (Ikornikova and Sheptunov 1973). For most of the carbonates the order is as follows:

$$\sim 470^{\circ}C\ T_{d\ FeCO3} < T_{d\ MgCO3} << T_{d\ ankerite} << T_{d\ dolomite} << T_{d\ calcite} \sim 900^{\circ}C$$

The thermal decomposition of magnesite occurs at the temperature range of 500–600ºC, while that of ankerite and dolomite occurs at 600–800ºC. The rounded to sub-rounded carbonates of Y-86029 are mainly ankeritic with minor amounts of siderite suggesting that some of the siderite may not have completely decomposed.

The sharp contact between the magnetite and enclosing carbonate suggests that they probably did not form contemporaneously. It appears that the carbonate was deposited on earlier formed magnetite with later deposition of dolomite in interstices. A few of these carbonates also contain sulfides. Co-precipitation of sulfide and carbonate has been determined to be thermodynamically favored under reducing conditions along the siderite-pyrite phase boundary with thermal decomposition accounting for the sulfide-related magnetite assemblage (Garrels and Christ 1965). Elongate morphologies of magnetite within carbonate in Y-86029 have also been observed in Y-82162 and have been

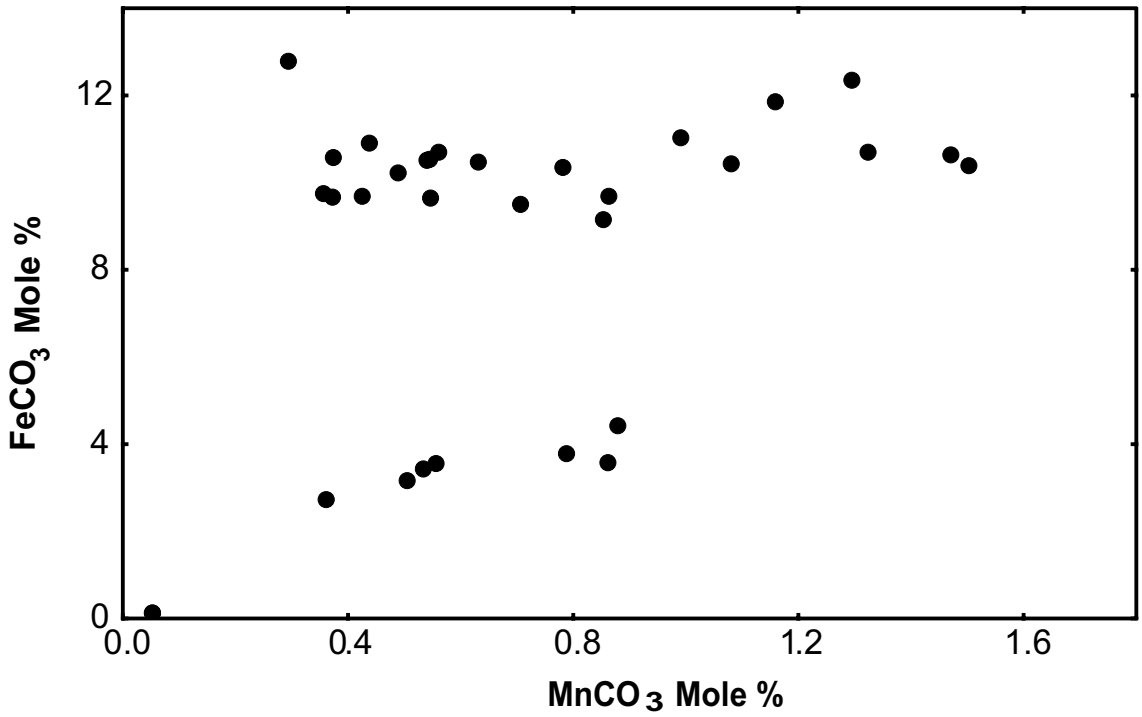

Fig. 16. Plot of Mn versus Fe contents (WDS data) in Y-86029 rounded to sub-rounded carbonates. No relationship is apparent.

interpreted as having resulted from heating of sulfides (Zolensky, Barrett, and Prinz 1989a). Hence, it is possible that this magnetite might have replaced a mixture of carbonate and sulfide.

The only other unusual carbonates described in CI chondrites are spherical 'amoeboid' carbonates with radiating crystal forms (Fredriksson and Kerridge 1988). These carbonates were interpreted to have resulted from growth under ambient conditions from an amorphous medium. Like the Y-86029 carbonates, these 'amoeboids' also contain magnetite. The presence of radiating crystals require the maintenance of a delicate balance between crystallization rate and the rate at which impurities can diffuse away from the growing crystal faces (Keith and Padden 1963, 1964; Lofgren 1971; Fredriksson and Kerridge 1988). The fine and uniform texture of the rounded to sub-rounded carbonates in Y-86029 argues for crystallization from a fluid circulating in interconnected pore spaces during the entire growth.

Large Periclase Clasts

Unusually large periclase clasts like those in Y-86029 have not been observed in carbonaceous chondrites. One possible explanation for the occurrence of periclase is that it may have resulted from dehydration of brucite, which is one of the products of serpentinization. However, formation of brucite as a result of serpentinization has rarely been observed in carbonaceous chondrites probably because of the low values of $f(O_2)$ required for serpentinization (Wicks and Plant 1979). Periclase can also react with water to produce brucite (Watanabe 1935; Wicks and Plant 1979), although this reaction is unlikely in Y-86029 because periclase is known to be stable in contact with H_2O only at temperatures above 900ºC, and fluid water at sufficient pressure to allow it to be converted to brucite must usually be present at some stage of metamorphism (Williams, Turner, and Gilbert 1982). The abundance of coarse phyllosilicates in Y-86029 suggests a lack of a late stage aqueous alteration, which would have provided the water for this reaction after thermal metamorphism. Periclase has also been described in Y-82162 where it occurs either as individual grains (generally <10 μm) or as finer-grained vein filling often intergrown with carbonates (Ikeda 1991; Lipschutz, Zolensky, and Bell 1999). We concur with these workers that the periclase most likely formed as a heating product of Mg-rich carbonate precursors. There is a general lack of experimental data on thermal decomposition of carbonate to periclase, and hence we can only propose hypotheses for its formation here.

The MgO/(MgO + FeO) molecular ratio of periclase, 0.50–0.56, in Y-86029 suggests that the original carbonates had similar ratios. We can postulate a simple model to explain periclase formation assuming that they formed from primary carbonates by heating. When the original $CaCO_3$-rich materials were heated, the carbonates decomposed into the mono-oxides with loss of CO_2. Magnesite and siderite components of the original carbonates decomposed to produce grains or fine-grained aggregates of the Fe-bearing periclase. Partial decomposition of Mg-Fe carbonates during further heating resulted in some of the MgO reacting with FeS

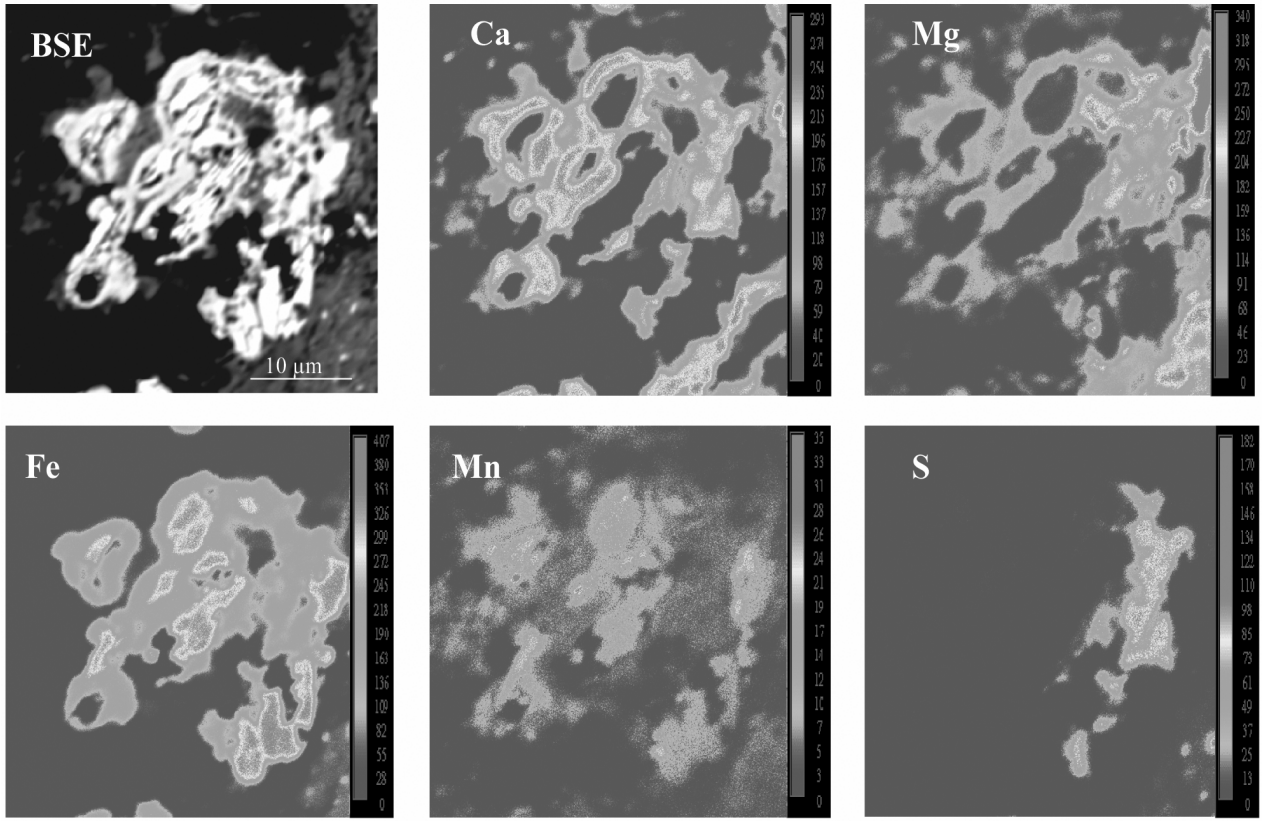

Fig. 17. BSE and element maps (Ca, Mg, Fe, Mn, and S) of the Y-86029 rounded to sub-rounded carbonates. Scale bar = 10 μm.

and incorporating FeS to periclase. This is evidenced by the presence of minute, fracture-filling sulfide grains in one of the large periclase aggregates. Heating of some Mg-Fe-Mn carbonates at this stage produced mixtures of periclase and MnO-rich, poorly crystalline oxides evident in the heated carbonate. The reaction of the carbonates with FeS also resulted in some of the rims evident in these carbonates.

The CO_2 fugacity of original materials during periclase formation is unclear. Ikeda (1991) proposed for Y-82162 that it must have been within a temperature range from 420 to 900 K. These values are satisfied by the thermal metamorphic temperatures experienced by Y-86029 and published thermodynamic data (e.g., Robie, Hemingway, and Fisher 1979). It also suggests that periclase formation took place in the parent body in highly oxidizing gas ($>10^{-4}$ bars). The fact that the periclase has not reacted with H_2O to produce brucite suggests that oxidizing conditions were favorable in Y-86029. The mechanism of formation of large carbonate precursors of periclase is also unclear, but there is no reason to believe that, like the rounded carbonates, they would have crystallized from ambient fluids in unrestricted pore spaces within the matrix.

Genetic Relationship Among Components and Other CI Chondrites

Matrix phyllosilicates in Y-86029 have similar fe# ratios as coarse phyllosilicates i.e., 0.15–0.52, suggesting that they formed under similar conditions. Magnetite must have also formed contemporaneously under similar conditions as shown by association with coarse phyllosilicates. The rounded to sub-rounded carbonates enclose magnetite, suggesting later formation. Some of the isolated carbonates in turn are rimmed by sulfides (mostly pyrrhotite), indicating a still later sulfidization event. It appears that this sulfidization was not pervasive as it affected only some components of the meteorite. Finally, isolated anhydrous aggregates were incorporated into Y-86029 after aqueous alteration.

Y-86029 and Y-82162 are the only naturally heated CI-like chondrites discovered so far. Apart from the unusual textures in Y-86029, the two meteorites show similar distribution of secondary minerals with minor exceptions. The sulfides have similar morphologies, i.e., euhedral, anhedral, and lath-like forms, and consist mainly of pyrrhotite and rarely pentlandite. However, Cu-Fe sulfide (cubanite) is present in Y-82162 (Tomeoka, Kojima, and Yanai 1989b; Ikeda 1991) and in non-Antarctic CI chondrites (MacDougall and Kerridge 1977) but not in Y-86029. Like Y-82162, sulfides seem more abundant in Y-86029 than in other CI chondrites (Zolensky, Barrett, and Prinz 1989a; Tomeoka, Kojima, and Yanai 1989b), probably as a result of availability of sulfur or thermal decomposition of originally Fe-Ni rich phyllosilicates. Magnetite is associated with the sulfides and

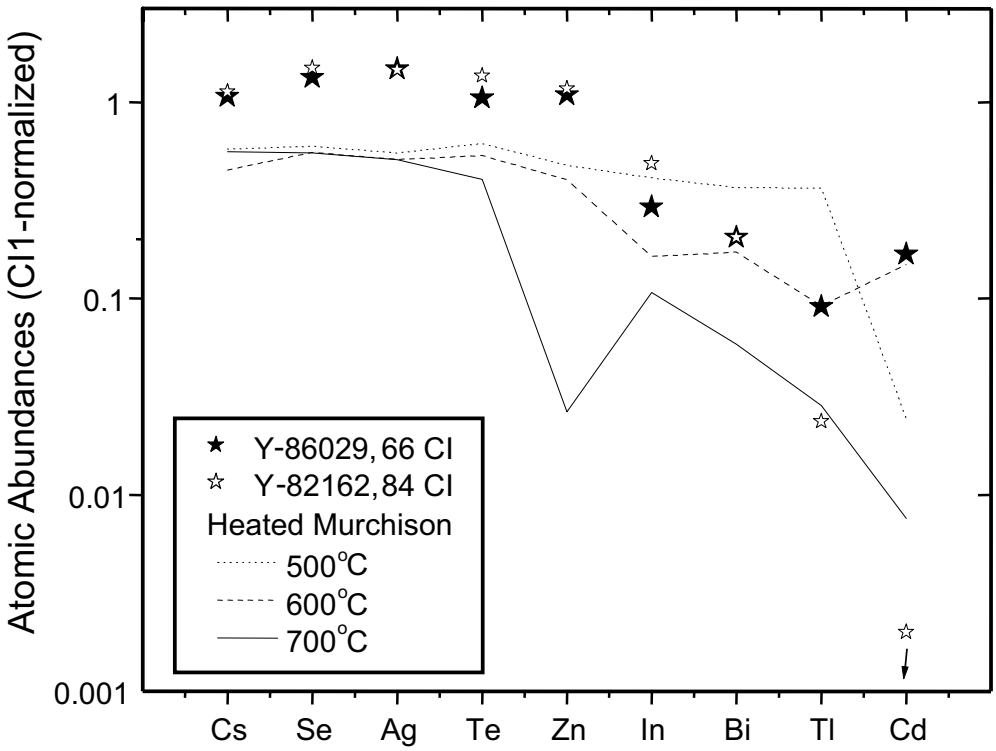

Fig. 18. Contents of 9 thermally mobile trace elements in Y-86029 and Y-82162 CI1 chondrites compared with data for a Murchison CM2 chondrite heated for one week at 500º, 600º, or 700ºC under ambient conditions simulating those during metamorphism of primitive parent objects. Elements are ordered from left to right by increasing degree and ease of loss at 600–700ºC during artificial heating. Data for the 9 elements in unheated CI1 and CM2 chondrites would define horizontal lines at 1.0 and lower values, respectively e.g., 0.62 ± 0.06 for Murchison (Xiao and Lipschutz 1992). The 4 most mobile elements (In → Cd) are clearly depleted in Y-82162 and Y-86029 relative to the 5 less-mobile ones. The two most mobile elements, Tl and Cd, are more depleted in Y-82162 than in Y-86029, arguing that the former was metamorphosed under more severe conditions than the latter. Comparison of data for the two CI1 chondrites with those of artificially heated Murchison suggests metamorphic temperatures of 500–600ºC for Y-86029 and 600–700ºC for Y-82162.

coarse phyllosilicates in the two meteorites although the sulfides often occur as rims in Y-82162.

The coarse and matrix phyllosilicates are also compositionally similar in the two meteorites and contain varying amounts of Fe as observed in most CI chondrites (Zolensky, Barrett, and Prinz 1989a; Tomeoka, Kojima, and Yanai 1989b). These phyllosilicates are mixtures of serpentine and smectite, although Ikeda (1991) proposed that they are mixtures of chlorite, serpentine, and saponite. Ferrihydrite has been reported in Y-82162 (Tomeoka and Buseck 1988) but not in Y-86029.

The matrix of Y-86029 is more homogeneous than that of Y-82162 as shown by the correlations between Fe, S, and Si and Ni with S. This correlation is absent in Y-82162 (Tomeoka, Kojima, and Yanai 1989b) and present in non-Antarctic (unmetamorphosed) CI chondrites. It is unclear why this relationship is absent in Y-82162; Mg/Fe ratios for matrix phyllosilicates in the two meteorites are similar to those for Orgueil. Phyllosilicate veins are present in Y-82162 and absent in Y-86029.

Similarities and differences occur between the two meteorites in the distribution of the carbonates. The dominant carbonates in Y-82162 are isolated grains of breunnerite and traces of dolomite, calcite, ankerite, and siderite (Ikeda 1991; Zolensky, Barrett, and Prinz 1989a; Tomeoka, Kojima, and Yanai 1989b). This is similar to the isolated carbonate grains in Y-86029, which are often rimmed by pyrrhotite and poorly crystalline Mn-Fe phases. Rounded to sub-rounded carbonates are present in Y-86029 and absent in all CI chondrites described to date.

Awaruite and whitlockite are also present as minor phases in Y-82162 and absent in Y-86029. Apatite is abundant in the two meteorites and shows a genetic relationship with coarse phyllosilicates, magnetite and carbonates. Anhydrous silicate grains are present in the two meteorites and all CI chondrites, and they appear to have been incorporated into these meteorites after the major aqueous alteration phase (Reid et al. 1970; Kerridge and McDougall 1976).

From the characteristics described, it is apparent that Y-82162 and Y-86029 underwent similar post-accretionary processes in their parent bodies with a few exceptions. The distribution of these components suggests that Y-82162 and Y-86029 were derived from similar asteroids, although not necessarily the same one.

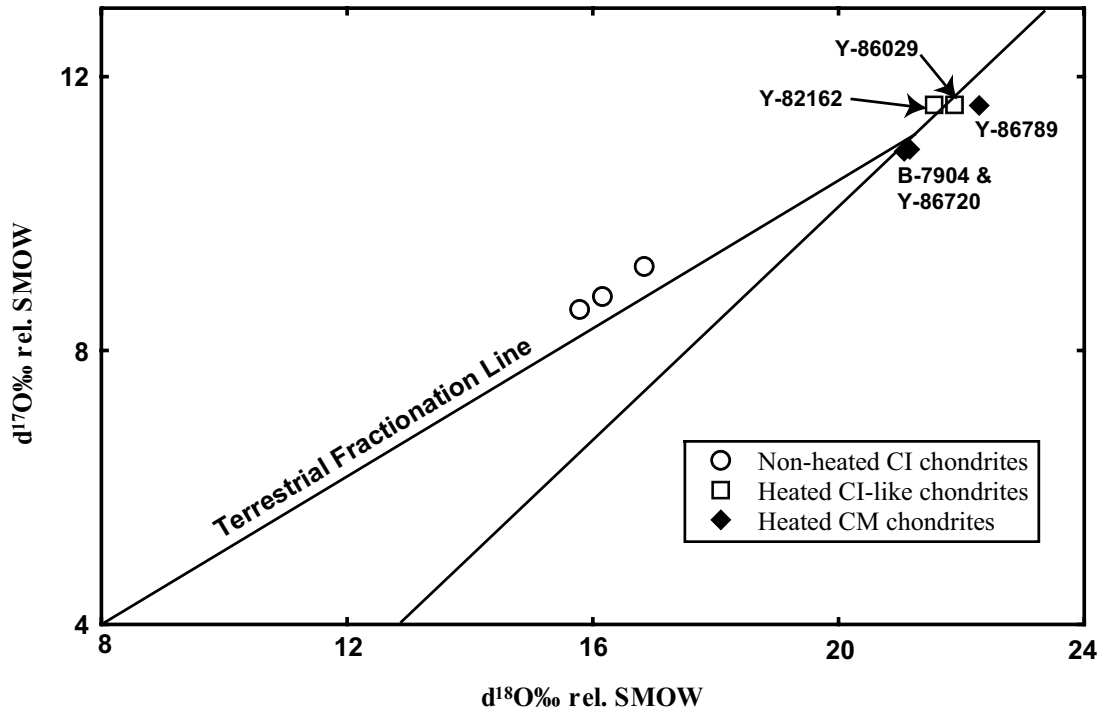

Fig. 19. Oxygen isotopic compositions of Y-86029 and Y-82162 compared with those for non-heated CI chondrites (Alais, Ivuna, and Orgueil) and thermally metamorphosed CM chondrites Y-86720, Y-86789, and B-7904 (data for other carbonaceous chondrites except Y-86029 obtained from Clayton and Mayeda 1999). The unlabelled line is the CO-CK-CM mixing line defined by Clayton and Mayeda (1999).

SUMMARY

Y-86029 is only the second thermally metamorphosed CI-like chondrite discovered so far. Mobile trace element chemistry suggests that it experienced moderate, open system heating (~500–600ºC). The most obvious petrographic evidence for this heating is in partial dehydration of phyllosilicates to olivine, the transformation proceeding via poorly crystalline 'intermediate phases' rarely found in meteorites. Y-86029 also contains unusual textures. Large (300–500 μm) periclase clasts are present, probably as a result of heating of Mg-Fe rich carbonate precursors under highly oxidizing gas conditions in the parent body. An isolated olivine aggregate in Y-86029 shows evidence for possible shock-induced melt recrystallization. This aggregate appears to be 'foreign' and was probably incorporated into Y-86029 from elsewhere in the parent asteroid (s) during the waning stages of asteroid erosion. Rounded to sub-rounded carbonates of ankerite/siderite compositions enclosing magnetite are also present. Formation of these carbonates by aqueous alteration at specific thermal decomposition temperatures appears to be satisfied in Y-86029. Despite similarities in distribution of secondary components, the presence of unusual textures in Y-86029 and differences in RNAA peak heating temperatures preclude its pairing with Y-82162. We believe that they were probably derived from similar asteroids rather than one asteroid.

Acknowledgments–This research has been carried out as part of the National Research Council (NRC) associateship award to Eric K. Tonui. Michael E. Zolensky is supported by a grant by NASA's Cosmochemistry Program. Michael E. Lipschutz also acknowledges with great appreciation the staff at the University of Missouri Research Reactor for aid in neutron irradiations, which were supported by DOE grant DE-FG07-01ID14146. Additional support for Michael E. Lipschutz was provided by NASA grant NAGW-3396. We are grateful to NIPR for providing thin sections of Y-86029 and Professor Y. Ikeda of Ibaraki University for useful counsel. We are also grateful to Craig Schwandt for his assistance with technical aspects of electron microprobe and SEM work. Critical reviews by Xin Hua and Matthieu Gounelle led to improvement in the manuscript. We acknowledge NIPR and the U.S. National Science Foundation for supporting the collection of Antarctic meteorites (via the Japanese Antarctic Research Expeditions, JARE, and the Antarctic Search for Meteorites, ANSMET) which continue to provide us with valuable samples for these studies.

REFERENCES

Akai J. 1988. Incompletely transformed serpentine-type phyllosilicates in the matrix of Antarctic CM chondrites. *Geochimica et Cosmochimica Acta* 52:1593–1599.

Akai J. 1990. Thermal metamorphism in four Antarctic carbonaceous chondrites and its temperature scale estimated by T-T-T diagram.

In *Antarctic Meteorites XV*. Tokyo: National Institute of Polar Research. pp. 86–87.

Anders E. and Grevesses N. 1989. Solar system abundances of the elements: Meteoritic and solar. *Geochimica et Cosmochimica Acta* 53:197–214.

Ashworth J. R. 1985. Transmission electron microscopy of L-group chondrites, 1. Natural shock effects. *Earth and Planetary Science Letters* 27:43–50.

Ball M. C. and Taylor H. F. W. 1963. The dehydration of chrysotile in air and under hydrothermal conditions. *Miner. Mag.* 33:467–482.

Bart M., Ikramuddin M., and Lipschutz M. E. 1980. Thermal metamorphism of primitive meteorites-IX. On the mechanism of trace element loss from Allende heated up to 1400°C. *Geochimica et Cosmochimica Acta* 44:719–730.

Bauer J. F. 1979. Experimental shock metamorphism of mono- and polycrystalline olivine: A comparative study. Proceedings, 10th Lunar and Planetary Science Conference. pp. 2573–2596.

Brearley A. J. 1997. Phyllosilicates in the matrix of the unique carbonaceous chondrite Lewis Cliff 85332 and possible implications for the aqueous alteration of CI chondrites. *Meteoritics & Planetary Science* 32:377–388.

Brearly A. J. and Prinz M. 1992. CI chondrite-like clasts in Nilpena polymict ureilite: Implications for aqueous alteration processes in CI chondrites. *Geochimica et Cosmochimica Acta* 56:1373–1386.

Brindley G. W. and Brown G. 1984. *Crystal structures of clay minerals and their x-ray identification.* London: Spottiswoode Ballantyne Ltd. pp. 495.

Brindley G. W. and Hayashi R. 1965. Mechanism of formation of forsterite and enstatite from serpentine. *Miner. Mag.* 35:189–195.

Brindley G. W. and Zussman J. 1957. Structural study of the thermal transformation of serpentine minerals to fosterite. *American Mineralogist* 42:461–474.

Bullock E. S., Gounelle M., Grady M. M., and Russell S. S. 2002. Fe-Ni sulfides in Tagish Lake and CI1 and CM2 chondrites (abstract #5141). 65th Annual Meeting of the Meteoritical Society.

Burnett D. S., Woolum D. S., Benjamin T. M., Rogers P. S., Duffy C. J., and Maggiore C. 1989. A test of the smoothness of the elemental abundances of carbonaceous chondrites. *Geochimica et Cosmochimica Acta* 53:471–481.

Clayton R. N. and Mayeda T. K. 1963. The use of bromine pentafluoride in extraction of oxygen from oxides and silicates for isotopic analysis. *Geochimica et Cosmochimica Acta* 27:43–52.

Clayton R. N. and Mayeda T. K. 1983. Oxygen isotopes in eucrites, howardites, nakhlites, and chassignites. *Earth and Planetary Science Letters* 62:1–6.

Clayton R. N. and Mayeda T. K. 1999. Oxygen isotope studies of carbonaceous chondrites. *Geochimica et Cosmochimica Acta* 63: 2089–2104.

Dennison J. E., Lingner D. W., and Lipschutz M. E. 1986. Antarctic and non-Antarctic meteorites form different populations. *Nature* 319:390–393.

Dodd R. T. and Jarosewich E. 1979. Incipient melting and shock classification of L group chondrites. *Earth and Planetary Science Letters* 44:335–340.

DuFresne E. R. and Anders E. 1962. On the chemical evolution of carbonaceous chondrites. *Geochimica et Cosmochimica Acta* 26: 1085–1114.

Fredriksson K., Jarosewich E., Beauchamp R., and Kerridge J. F. 1980. Sulphate veins, carbonates, limonite, and magnetite: Evidence on the late geochemistry of the C-1 regoliths. *Meteoritics* 15:291–292.

Fredriksson K. and Kerridge J. F. 1988. Carbonates and sulfates in CI chondrites: Formation by aqueous activity on the parent body. *Meteoritics & Planetary Science* 23:35–44.

Friedrich J. M., Wang M. S., and Lipschutz M. E. 2002. Comparison of the trace element composition of Tagish Lake with other primitive carbonaceous chondrites. *Meteoritics & Planetary Science* 37:677–686.

Gandolfi G. 1967. Discussion upon methods to obtain x-ray powder patterns from a single crystal. *Miner. Petrogr. Acta* 13:67–74.

Garrels R. M. and Christ C. L. 1965. *Solutions, minerals, and equilibria.* New York: Harper and Row. p. 450.

Golden D. C., Ming D. W., Schwandt C. S., Lauer H. V., Socki R. A., Morris R. V., Lofgren G. E., and McKay G. A. 2001. A simple inorganic process for formation of carbonates, magnetite, and sulfides in Martian meteorite ALH84001. *American Mineralogist* 86:370–375.

Goldstein J. I. 1979. Principles of thin-film x-ray microanalysis. In *Introduction to Analytical Electron Microscopy*, edited by Hren J. J. et al. New York: Plenum Press. pp. 813–820.

Gounelle M. and Zolensky M. E. 2001. A terrestrial origin for sulfate veins in CI chondrites. *Meteoritics & Planetary Science* 36: 1321–1329.

Hiroi T., Pieters C. M., Zolensky M. E., and Lipschutz M. E. 1993. Evidence of thermal metamorphism on C, G, B, and F asteroids. *Science* 261:1016–1018.

Hiroi T., Pieters C. M., Zolensky M. E., and Lipschutz M. E. 1994. Possible thermal metamorphism on the C, B, and F asteroids seen from the 0.7-μm, 3-μm, and UV absorption strengths in comparison with carbonaceous chondrites. *Meteoritics & Planetary Science* 31:321–327.

Hiroi T., Pieters C. M., Zolensky M. E., and Lipschutz M. E. 1996. Thermal metamorphism of the C, G, G, B, and F asteroids seen from the 0.7-μm, 3--μm, and UV absorption strengths in comparison with carbonaceous meteorites. *Meteoritics & Planetary Science* 31:321–327.

Ikeda Y. 1991. Petrology and mineralogy of the Yamato-82162 chondrite (CI). Proceedings, 4th NIPR Symposium on Antarctic Meteorites. pp. 187–225.

Ikornikova A. and Sheptunov D. 1973. Dissociation curves of trigonal carbonates. In *Crystallization processes under hydrothermal conditions*, edited by Lobachev A. N. New York: Consultants Bureau. pp. 113–123.

Ikramuddin M. and Lipschutz M. E. 1975. Thermal metamorphism of primitive meteorites-I. Variation of six elements in Allende carbonaceous chondrite heated at 400–1000°C. *Geochimica et Cosmochimica Acta* 57:439–452.

Jedwab J. 1971. La magnetite en plaquettes d'Orgueil vue au microscope electronique a Balayage. *Icarus* 35:319–340.

Keith H. D. and Padden F. J. 1963. A phenomenological theory of spherulitic crystallization. *Journal of Applied Physics* 34:2409.

Keith H. D. and Padden F. J. 1964. Spherulitic crystallization from the melt, 1. Fractionation and impurity segregation and their influence on crystalline morphology. *Journal of Applied Physics* 35:1270.

Kerridge J. F. and McDougall J. D. 1976. Mafic silicates in the Orgueil carbonaceous meteorite. *Earth and Planetary Science Letters* 29:341–348.

Kerridge J. F., Mackay A. L., and Boynton W. V. 1979. Magnetite in CI carbonaceous meteorites: Origin by aqueous activity on a planetesimal surface. *Science* 205:395–397.

Lipschutz M. E., Zolensky M. E., and Bell M. S. 1999. New petrographic and trace element data on thermally metamorphosed carbonaceous chondrites. Proceedings, 12th NIPR Symposium on Antarctic Meteorites. pp. 57–80.

Lofgren G. 1971. Spherulitic textures in glassy and crystalline rocks.

Journal of Geophysical Research 76:5635–5648.
MacDougall J. D. and Kerridge J. F. 1977. Cubanite: A new sulfide phase in CI meteorites. *Science* 197:561–562
Matza S. D. and Lipschutz M. E. 1977. Thermal metamorphism of primitive meteorites VI. Eleven trace elements in Murchison C2 chondrite heated at 400–1000°C. Proceedings, 8th Lunar and Planetary Science Conference. pp. 161–176.
Mayeda T. and Clayton R. 1990. Oxygen isotopic compositions of B-7904, Y-82162, and Y-86720. Proceedings, 15th NIPR Symposium on Antarctic Meteorites. pp. 89–91.
McGarvie D. W., Wright I. P., Grady M. M., Pillinger C. T., and Gibson E. K., Jr. 1987. A stable carbon isotopic study of types 1 and 2 carbonaceous chondrites. *Memoirs of the National Institute of Polar Research* 46:179–195.
McSween H. Y. and Richardson S. M. 1977. The composition of carbonaceous chondrite matrix. *Geochimica et Cosmochimica Acta* 41:1145–1161.
Nagy B. and Andersen C. A. 1964. Electron probe microanalysis of some carbonate, sulfate, and phosphate minerals in the Orgueil meteorite. *American Minerologist* 49:1730–1736.
Nakamura T., Noguchi T., Yada T., Nakamuta Y., and Takaoka N. 2001. Bulk mineralogy of individual micrometeorites determined by x-ray diffraction analysis and transmission electron microscopy. *Geochimica et Cosmochimoca Acta* 65: 4385–4397.
Ngo H. T. and Lipschutz M. E. 1980. Thermal metamorphism of primitive meteorites-X. Additional trace elements in Allende (CV3) heated to 1400°C. *Geochimica et Cosmochimica Acta* 44: 731–739.
Paul R. L. and Lipschutz M. E. 1989. Labile trace elements in some Antarctic carbonaceous chondrites: Antarctic and non-Antarctic meteorite comparisons. *Zeitschrift für Naturforschung* 44a:979–987.
Paul R. L. and Lipschutz M. E. 1990. Consortium study of labile trace elements in some Antarctic carbonaceous chondrites: Antarctic and non-Antarctic meteorite comparisons. Proceedings, 3rd NIPR Symposium on Antarctic Meteorites. pp. 80–95.
Reid A. M., Bass M. N., Fujita H., Kerridge J. F., and Fredriksson K. 1970. Olivine and pyroxene in the Orgueil meteorite. *American Minerologist* 49:1730–1736.
Reimold W. U. and Stöffler D. 1978. Experimental shock metamorphism of dunite. Proceedings, 9th Lunar and Planetary Science Conference. pp. 2805–2824.
Robie R. A., Hemingway B. S., and Fisher J. R. 1979. Thermodynamic properties of minerals and related substances at 298. 15K and 1 bar (105 Pascals) pressure and at higher temperatures. *Geological Survey Bulletin* 1452:456.
Richardson S. M. 1981. Alteration of mesostasis in chondrules and aggregates from three C2 carbonaceous chondrites. *Earth and Planetary Science Letters* 52:67–75.
Schreyer W., Abraham K., and Kulke H. 1980. Natural sodium phlogopite coexisting with potassium phlogopite and sodian aluminium talc in a metamorphic evaporite sequence from Derrag, Tell Atlas, Algeria. *Contributions to Mineralogy and Petrology* 74:223–233.
Scott E. R. D. 1988. A new kind of primitive chondrite, Allan Hills 85085. *Earth and Planetary Science Letters* 91:1–18.
Scott E. R. D., Keil K., and Stöffler D. 1992. Shock metamorphism of carbonaceous chondrites. *Geochimica et Cosmochimica Acta* 56:4281–4293.
Stöffler D., Keil K., and Scott E. R. D. 1991. Shock metamorphism of ordinary chondrites. *Geochimica et Cosmochimica Acta* 55: 3845–3867.
Takeda H., Wooden J. L., Mori H., Delaney J. S., Prinz M., and Nyquist L. E. 1983. Comparison of Yamato and Victoria Land polymict eucrites: A view from mineralogical and isotopic studies. Proceedings, 14th Lunar and Planetary Science Conference. *Journal of Geophysical Reserach* 88:B245–B256.
Tomeoka K. 1990b. Phyllosilicate veins in a CI meteorite: Evidence for aqueous alteration on the parent body. *Nature* 345:138–140.
Tomeoka K. and Buseck P. R. 1988. Matrix mineralogy of the Orgueil CI carbonaceous chondrite. *Geochimica et Cosmochimica Acta* 52:1627–1640.
Tomeoka K., Kojima H., and Yanai K. 1989a. Yamato-86720: A CM carbonaceous chondrite having experienced extensive aqueous alteration and thermal metamorphism. Proceedings, 2nd NIPR Symposium on Antarctic Meteorites. pp. 55–74.
Tomeoka K., Kojima H., and Yanai K. 1989b. Yamato-82162: A new kind of CI carbonaceous chondrite from Antarctica. Proceedings, 2nd NIPR Symposium on Antarctic Meteorites. pp. 36–54.
Tonui E. K., Zolensky, M. E., and Lipschutz M. E. 2002a. Petrography, mineralogy, and trace element chemistry of Y-86029, LEW-85332, and Y-793321: Aqueous alteration and heating events. *Antarctic Meteorites Research* 15:38–58.
Tonui E. K., Zolensky M. E., Hiroi T., Lipschutz M. E., and Okudaira K. 2002b. Petrographic, chemical, and spectroscopic data on thermally metamorphosed carbonaceous chondrites (abstract #1288). 33rd Lunar and Planetary Science Conference. CD-ROM.
Valley J. W., Eiler J. M., Graham C. M., Gibson E. K Jr., Romanek C. S., and Stolper E. M. 1997. Low temperature carbonate concretions in the Martian meteorite ALH84001: Evidence for stable isotope mineralogy. *Science* 275:1633–1638.
Van der Brogert C. H., Schultz P. H., and Spray J. G. 2001. Impact darkening via high strain-rate deformation during impact: Spectral and chemical analyses (abstract #2167). 32nd Lunar and Planetary Science Conference. CD-ROM.
Wang M. S. and Lipschutz M. E. 1998. Thermally metamorphosed carbonaceous chondrites from data for thermally mobile trace elements. *Meteoritics & Planetary Science* 33:1297–1302.
Wang M. S., Socki R., Zolensky M. E., and Lipschutz M. E. 1998. Thermal metamorphism of carbonaceous chondrites: Simulations and reality. *Meteoritics & Planetary Science* 33: A161–162.
Wang M. S., Zolensky M. E., and Lipschutz M. E. 2000. Artificial heating of Ivuna and Murchison: Closed and open systems (unpublished).
Watanabe T. 1935. On the brucite-marble (predazzite) from the Nantei mine, Suian, Tyosen (Korea). *Journal of the Faculty of Science, Hokkaido Imperial University.* Series 4, volume 3. pp. 49–67.
Weisberg M. K., Prinz M., and Nehru C. E. 1988. Petrology of ALH 85085: A chondrite with unique characteristics. *Earth and Planetary Science Letters* 91:19–32.
Wicks F. J. and Plant G. 1979. Electron microscope and x-ray microbeam studies of serpentine textures. *Canadian Mineralogist* 17:785–830.
Williams H., Turner F. J., and Gilbert C. M. 1982. *Petrography: An introduction to study of rocks in thin sections*. 2nd edition. San Francisco: W. H. Freeman and Company.
Woods T. L. and Garrels R. M. 1992. Calculated aqueous-solution-solid-solution relations in the low temperature system CaO-MgO-FeO-CO_2-H_2O. *Geochimica et Cosmochimica Acta* 56: 3031–3043.
Zolensky M. E., Barrett R. A., and Prinz M. 1989a. Petrography, mineralogy, and matrix composition of Yamato-82162, a new CI2 chondrite. 20th Lunar and Planetary Science Conference. pp. 1253–1254.
Zolensky M. E. and McSween H. Y. 1988. Aqueous alteration. In *Meteorites and the Early Solar System*, edited by Kerridge J. F. and Mathews M. S. Tucson: University of Arizona Press.

Zolensky M. E., Barrett R. A., and Prinz M. 1989b. Mineralogy and petrology of Yamato 86720 and Belgica-7904. *Antarctic Meteorites* 14:24–26.

Zolensky M. E., Bourcier W. L., and Gooding J. L. 1989c. Aqueous alteration on the hydrated asteroids: Results of EQ3/6 computer simulations. *Icarus* 78:411–425.

Zolensky M. E., Barrett R. A., and Browning L. 1993. Mineralogy and composition of matrix and chondrule rims in carbonaceous chondrites. *Geochimica et Cosmochimica Acta* 57:3123–3148.

Zolensky M. E., Ivanov A. V., Yang V., and Ohsumi K. 1996. The Kaidun meteorite: Mineralogy of an unusual CM1 clast. *Meteoritics & Planetary Science* 31:484–493.

Zolensky M. E., Nakamura K., Gounelle M., Mikouchi T., Kasama T., Tachikawa O., and Tonui E. 2002. Tagish Lake: An ungrouped type 2 carbonaceous chondrite. *Meteoritics & Planetary Science* 37:737–761.